6-21-2012 12:00 AM

Experimental Evaluation of the Projection-based Force Reflection Algorithms for Haptic Interaction with Virtual Environment

Mir Z. Hasan
The University of Western Ontario

Supervisor
Dr. Ilia G. Polushin
The University of Western Ontario

Graduate Program in Electrical and Computer Engineering
A thesis submitted in partial fulfillment of the requirements for the degree in Master of Engineering Science

EXPERIMENTAL EVALUATION OF THE PROJECTION-BASED FORCE REFLECTION ALGORITHMS FOR HAPTIC INTERACTION WITH VIRTUAL ENVIRONMENT

(Spine title: Experimental Evaluation of the PFRA for Haptic Interfaces)

(Thesis format: Monograph)

by

Mir Zayed Hasan

Graduate Program in Electrical and Computer Engineering

A thesis submitted in partial fulfillment
of the requirements for the degree of
Master of Engineering Science

The School of Graduate and Postdoctoral Studies
The University of Western Ontario
London, Ontario, Canada

THE UNIVERSITY OF WESTERN ONTARIO
School of Graduate and Postdoctoral Studies

CERTIFICATE OF EXAMINATION

Supervisor:

. . . .
Dr. I. Polushin

Supervisory Committee:

Examiners:

. . . .
Dr. R. V. Patel

. . . .
Dr. Q. M. Rahman

. . . .
Dr. O. R. Tutunea-Fatan

The thesis by

Mir Zayed Hasan

entitled:

Experimental Evaluation of the Projection-based Force Reflection Algorithms for Haptic Interaction with Virtual Environment

is accepted in partial fulfilment of the
requirements for the degree of
Master of Engineering Science

. . . .
Date

. . . .
Chair of the Thesis Examination Board

Abstract

Haptic interaction with virtual environments is currently a major and growing area of research with a number of emerging applications, particularly in the field of robotics. Digital implementation of the virtual environments, however, introduces errors which may result in instability of the haptic displays. This thesis deals with experimental investigation of the Projection-Based Force Reflection Algorithms (PFRAs) for haptic interaction with virtual environments, focusing on their performance in terms of stability and transparency. Experiments were performed to compare the PFRA in terms of performance for both non-delayed and delayed haptic interactions with more conventional haptic rendering methods, such as the Virtual Coupling (VC) and Wave Variables (WV). The results demonstrated that the PFRA is more stable, guarantees higher levels of transparency, and is less sensitive to decrease in update rates.

Keywords: Haptic Systems, Projection based Force Reflection Algorithm

Acknowledgement

I would like to express my sincere appreciation and gratitude to my supervisor, Dr. Ilia G. Polushin, Assistant Professor, Department of Electrical and Computer Engineering, Western University, for his guidance, advice, assistance and encouragement throughout my research work.

I would like to express my thanks to Mr. Amir Takhmar, PhD student, Department of Electrical and Computer Engineering, Western University, for his assistance in modelling the haptic device. I would also like to extend my thanks to my friends in the Robotics and Control Laboratory for their help throughout the time I worked on my research.

I am especially grateful to my wife, Mrs. Qamrun Nahar, for her moral support and encouragement during the work.

Finally, I would like to express my gratitude to my parents, Mr. Mir Moazzem Hossain and Mrs. Mahbuba Morshed, for their love and support throughout my life.

Contents

List of Figures

List of Tables

List of Acronyms

PFRA: Projection based Force Reflection Algorithm
DFR: Direct Force Reflection
VC: Virtual Coupling
WV: Wave Variables
DOF: Degree of Freedom

Chapter 1

Introduction

1.1 Introduction

According to Robot Institute of America (RIA), the official definition of a robot is as follows [3]:

A robot is a reprogrammable manipulator designed to move materials, parts, tools, or specialized devices through variable programmed motion for the performance of a variety of tasks.

However, in the current context of robotics, this definition, while representing several inherent qualities of a robot, has become severely restricted. A robot can now be remotely controlled to perform exploration in undersea environments and in space, conveys information about a remote location to a user and can be used as a tool to perform surgical operations. Telerobotics has revolutionized the applicability of robots in a wide variety of fields. One of the major requirements of a telerobot is to convey information about the nature (texture, stiffness, color, temperature, etc.) of a remote environment to the user.

The human sense organs accept information about the surrounding environment for processing by the brain. In a similar manner, visual, auditory, haptic, olfactory and gustatory displays provide means of interaction between humans and virtual environments created by a computer system. While focus has been primarily on developing visual and auditory displays, haptics has the potential to improve the human-computer interaction by introducing the sense of touch. In the last decade, haptics has found application in molecular docking, manipulation of nano-materials, surgical training, virtual prototyping, and digital sculpting, among other areas. Haptics has enabled the active exploration of the virtual world [4].

1.2 Haptics

Haptics originates from the Greek word *haptikos*, which means 'to grasp'or 'perceive', and was coined by psychophysicists to label the subfield of their study in human touch based perception and manipulation. Since the 1970s, in the field of robotics, it refers to the modality of touch and may include sense of heat and surface texture of an object. Haptic perception ranges from minor interactions in everyday life to social communications. Researchers in the field of haptics are engaged in the development of devices and associated software that allow users to sense and interact with three dimensional objects rendered in the virtual environment. Haptics can be used to improve the users' experience during interaction with the virtual environment in the following aspects [5]:

a) Improved usability;

b) Enhanced realism;

c) Restoration of mechanical feel.

The sense of touch can distinguish between surface structures. Although skin is the most sensitive organ, additional receptors for haptic perception are located within muscles and joints. These receptors provide kinaesthetic perception while those located on the skin provide tactile perception. Tactile receptors can perceive forces with magnitudes in the range from 5mN to 5N, detect surface textures with small variations from 1μm to 1mm, and discriminate frequencies ranging from 10Hz to 1000Hz, while kinaesthetic receptors can detect much larger forces with frequencies usually not higher than 10Hz [6]. The combination of the responses from these two types of receptors allows humans to perform coordinated movements and interact with their surrounding environment.

A wide variety of haptic devices have been designed based on their area of application and the principle of operation. Force feedback techniques have received particular attention from researchers. An alternative approach to force feedback is vibrotactile display where multiple small forces are applied to the fingertips. Another technique to create a haptic perception is to use a temperature display where both environmental temperature and the sensation of heat or cold generated when grasping or colliding with an object can be simulated. One more type of device is the 2D haptic device where 2DOF force feedback planar device can be moved by the user to interact with edges of shapes in images.

1.2.1 Architecture of Virtual Reality Simulation

In order to simulate real or imaginary scenes that users can interact with, virtual reality (VR) applications allow humans to use their senses to discern and experience different properties of the virtual environment. Usually a subset of these senses are used, typically visual, auditory and touch are incorporated in such systems. A basic VR application has the following elements [7]:

a) Simulation engine;

b) Visual, auditory and haptic rendering algorithms;

c) Transducers.

Haptic perception is achieved when the user holds or wears a haptic device, which conveys information related to interaction with the virtual environment. While audio and video feedback is unidirectional from the engine to the user, haptic communication is bidirectional.

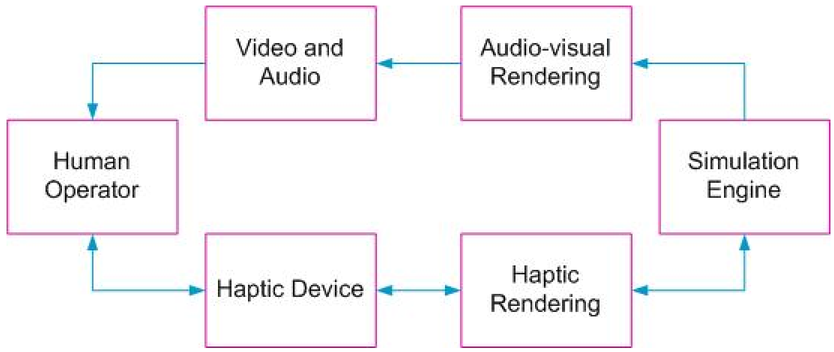

Figure 1.1: A basic architecture for virtual reality application incorporating audio, visual and haptic feedback [7]

1.2.2 Haptic Interface Devices

Haptic interface devices typically behave like small robots that directly interact with the human operator. They can be classified based on various features [7]:

a) Grounding locations, e.g. force feedback gloves and ground based devices;

b) Intrinsic mechanical behaviour: impedance and admittance;

c) Number of degree-of-freedom (DOF): number of possible dimensions of movement or force exchange.

In order to successfully represent touch and generate haptic perception, all haptic devices are expected to have the following desirable characteristics [7]:

a) Low back drive inertia;

b) Minimal constraints;

c) Symmetric inertia, friction, stiffness and frequency response;

d) Proper ergonomics.

Figure 1.2: Examples of haptic interface devices currently in use and research (clockwise from top left): Human exoskeleton [8], Haptic glove [9], Haptic joystick [10], and Pen-based master [11]

1.2.3 Haptic Rendering Algorithms

The haptic interface is represented by an avatar in the virtual environment, and all interactions with the environment are carried out by it. Contact between the avatar and the virtual environment create action and reaction forces. These forces are computed by the haptic rendering algorithms. Such an algorithm has the following components [7]:

a) Collision detection algorithms which detect collisions between the objects and the avatar, also generating information about the location, the time and the extent of the collision

b) Force-response algorithms generate the interaction force using the information from the collision detection algorithm

c) Control algorithms minimize the error between the ideal and the actual forces

The following sequence of events constitute a haptic loop [7]:

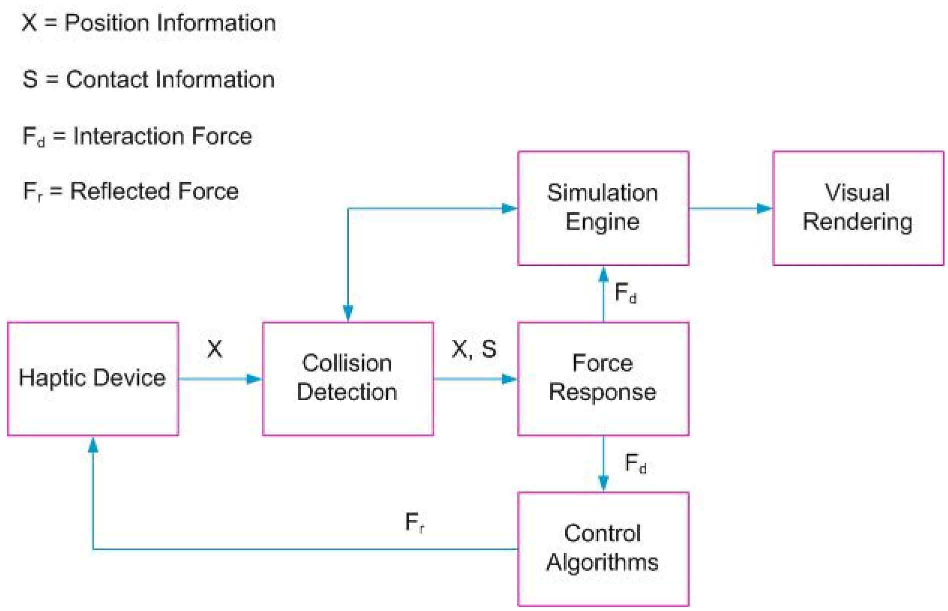

Figure 1.3: The basic blocks of a haptic rendering algorithm [7]

a) The joint positions are obtained;

b) The avatar's position is calculated by the forward kinematics algorithm;

c) The collision detection algorithm uses the position information to determine collisions and the degree of penetration;

d) The forces between the avatar and virtual objects are calculated;

e) The calculated forces are then applied by the control algorithm though the haptic device to the user while maintaining stability

While there is no fixed rule to determine the rate at which the force rendering algorithms update the computation, a rate of 1kHz is common, as it allows the presentation of reasonably complex objects with reasonably high stiffnesses. Two types of force rendering algorithms can be used [7]:

a) Geometry dependant force rendering algorithms: The interaction forces considered here are dependant on the geometry of the object, its compliance and the geometry of the avatar. A simple version of this algorithm measures the position of the operator and applies the forces to the operator along one spatial direction. When rendering a virtual wall, due to the discrete nature of haptic interaction, there will always be a penetration into the wall. This information can be used to compute the interaction force. A simple algorithm to render the virtual wall using this algorithm will be given by,

$$F = \begin{cases} 0 & x > x_w \\ K(x_w - x) & x \leq x_w \end{cases} \tag{1.1}$$

where, x describes the position of the avatar of the haptic device and x_w is the

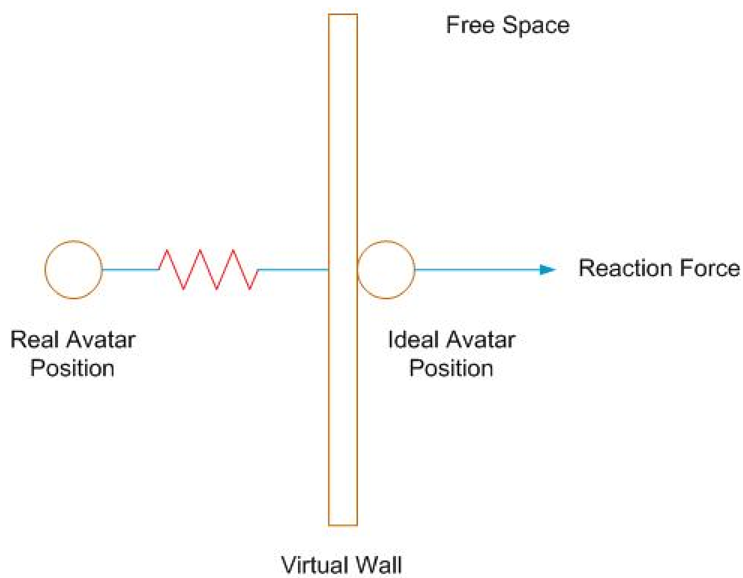

Figure 1.4: Virtual wall concept depicting a 1DOF interaction [7]

position of the virtual wall, and $K \geq 0$ represents the stiffness of the wall.

More complex versions of this algorithm include algorithms to calculate forces in 2DOF as in the case of a mouse interacting with a PC, 3DOF interaction using the point interaction paradigm, or more complex interactions with higher number of DOF.

b) Surface property dependant force-rendering algorithms: The second type of algorithms used to render forces in haptics utilizes information from tactile displays and therefore are dependant on the nature of the surface of the object being interacted with. Micro irregularities in the surface act as obstructions and cause friction when two such surfaces come into contact. While the model of friction is a complicated one, simpler, empirical models proposed by Leonardo da Vinci and developed by Coulomb are used in 3DOF as a basis for simple frictional models [7]. More accurate models exist, however, they typically require higher amount of computations and may be unsuitable for real time implementation.

1.2.4 Application Areas of Haptics

a) **Surgical Simulation and Medical Training:** This is an important application area for haptics. Haptic devices have found their use in training simulations for palpation of subsurface liver tumours, echographic examination of human thigh, for bone marrow harvest for transplant, for arthroscopic surgery, for simulation of fluid filled objects to explain different surgical procedures, for simulation of organ motion, devices for surgical teleoperation, and in medical training simulators used to gain baseline information about trainees.

b) **Museum Displays:** Using digital media and in-house kiosks, museums are exploring the possibility of creating 3D digital representations of their collections that visitors can not only see but also touch to appreciate. This can also allow curatorial staff to interact with people at a remote location in joint tactile exploration of works of art.

c) **Painting, Sculpting and CAD:** Haptic Displays have been used as an alternative input device for painting, sculpting, and CAD. Techniques have been developed to study the texture of fabric, to aid visually impaired people in painting, to edit animations, for 3D sculpting and geometric modelling.

d) **Visualization:** Scientific visualization has also benefited from incorporating haptic systems. Haptics and graphic displays have been combined in computation software steering systems. Haptics have also been incorporated in software to analyse chemical and biological molecular structures.

e) **Military Applications:** Aerospace and military training and simulation have also taken advantage of developments in haptics. Force feedback gloves have been used by workers at remote locations to simulate the reconfiguration of a vehicle by handling different virtual components. NASA has been carrying out experiments in the psychophysical field to study the effects of attaching a 3DOF manipulandum to a visual display. Adding haptics to audio and visual display allows for an increase in situation awareness, providing accurate orientation information in land, sea and aerospace environments.

f) **Interaction Techniques:** Haptics has also been applied to user interface, where force feedback can give the user a more realistic feeling of interacting with an interface, such as pressing a button. Objects can be rendered with Javascript and can be delivered for exploration using haptic mice via a standard webpage. Haptic gloves have been used to provide users a more realistic feel of stacking or pushing objects. Haptics have also been used by system designers to guide users along a right path, by adding built-in force constraints along the wrong path or against wrong choices.

g) **Assistive Technology for Disabled Persons:** Visually impaired people can benefit from incorporating haptics in assistive technology. Computer user interfaces have been haptically modified to identify edges of icons or windows. Software have also been developed to aid people with such disabilities to identify objects with simple shapes. Haptic displays have also been used to allow people to feel the shape of mathematical curves or play simple games such as battleship. People with disabilities related to stroke have also benefited from the use of haptics in rehabilitation program where movement exercises in virtual reality allow them to move objects of defined size and weight from one place to the other.

1.3 Literature Survey

1.3.1 Virtual Coupling

When a unilateral constraint like a virtual wall is simulated, a demand is placed on the requirements of the range of impedance that the haptic display can render, known as the z-width, with the ideal dynamic range of it varying from near zero to near infinite. However, such a wide range of impedances is not possible to simulate without the loss of stability. Colgate, et. al., [12] proposed the concept of virtual coupling to overcome this problem. In this work, the virtual tool and the environment are implemented in a way to guarantee that they are discrete time passive. Specifically, the handle of the virtual tool is connected to the handle of the haptic display via a multidimensional coupling consisting of stiffness and damping. The virtual coupling effectively limits the maximum impedance exhibited by the haptic display, even when the impedance of the virtual wall is infinite.

Adams and Hannaford [13, 14] extended the concept of virtual coupling from the impedance model in [12] to the admittance model of haptic interaction. They represented the coupling in the admittance display as a frequency dependent damper, which has a zero steady state impedance, while an effective damping at high frequency created by the impedance of the mass that becomes dominant at those frequencies. Their analysis showed that the virtual coupling network design is independent of the impedance or admittance causality of the virtual environment model, if the environment is passive. They also showed that the two port networks arising from the admittance and impedance displays are dual.

In [15, 16], the authors used Excalibur, a three degree of freedom Cartesian manipulator designed to act as a haptic interface, and Virtual Building Block system, which is a haptic simulation, to design stabilizing haptic interface control laws for a large z-width. They implemented two variations of the virtual coupling: the impedance display and the admittance display. Their experimental results showed that the impedance display is very simple but not as adaptable as an admittance display.

Miller, et. al., [17] addressed the question of ensuring stability in nonpassive nonlinear environments in both delayed and nondelayed form for haptic systems consisting of four components: human, haptic device, virtual coupling and virtual environment. The authors derived design conditions that guarantee the velocity signal from the device to the human goes to zero in the steady state and all states are bounded. This would ensure that any undesirable velocity signal resulting from oscillatory motion can not be presented to the user. They also considered a general device model that is exact.

Lertpolpairoj, et. al., [18] modified the concept of virtual coupling presented in [12]. The authors adapted the values of stiffness and damping of the coupling depending on the parameter called Interacting Frequency. Their experiments showed that the adaptive virtual coupling was identical to the static virtual coupling for virtual environments with low stiffness values. But when the virtual environment has a high value of stiffness, the adaptive virtual coupling system represented the impedances better.

In [19], Lee and Lee presented a new model for stability analysis of the haptic device. They modelled the human arm as a linear time-invariant (LTI) 2nd order impedance and a response model. A nonlinear virtual coupling is developed to maximize the impedance of the virtual coupling and to derive the stability condition. The stability condition proposed by the authors is less conservative than the passivity condition. Their results showed that the new stability condition increased the upper bound of achievable stiffness and damping compared to the passivity condition. When combined with a nonlinear version of virtual coupling, the results proved even more satisfactory. In this case the authors designed the virtual coupling as a piecemeal linear model, with each portion having a different stiffness.

Bi, et.al. [20], used fuzzy logic to adapt the parameters of the virtual coupling in order to improve its performance. Their results showed that the fuzzy logic based adaptive virtual coupling produced very little overshoot in displacement when interacting with virtual environments, as compared to traditional virtual coupling. Also, the speed of response is improved while maintaining the primary objective of stabilizing the a haptic display.

In [21], Akahane, et. al., used virtual coupling to interface between a virtual environment and a High Definition Haptic Controller. The controller achieves a 10kHz high definition haptic rendering in a 3DOF haptic interface, which has a z-width almost ten times that of a 1kHz rendering. An analytical method is used by the authors that allows for stable rendering of a hard surface. For a Virtual Reality application to maintain a video rate control frequency to provide visual sensation, the virtual environment is rendered at 60Hz. As the haptic display is an impedance display rendered at 10kHz and the virtual environment is an admittance display rendered at 60Hz, the authors used a virtual coupling process, for up sampling and as an interface between the components. The system achieved stability of the haptic system with a virtual coupling of low impedance while maintaining high fidelity with the 10kHz high definition haptic rendering with a high interpolating impedance.

Questions on position coherency in network haptic virtual environment (NHVE) are addressed in [22]. The authors designed three virtual coupling schemes: two peer-to-peer and one client-server model, to maintain position coherency. They did not use any time delay compensation method. In the peer-to-peer schemes, a model of the mass is implemented at each user, while the mass was modelled only at the server in the client-server model. When there were only two users, the preliminary results presented by the authors showed that the client-server model of the virtual coupling scheme had the lowest peak and RMS position error. However, their analysis also showed that this model had the largest delay among the three models. In [23], the authors carried out experiments using the three virtual coupling schemes over the internet. Of the three experiments carried out, two used the same scheme but the parameters of the virtual coupling were changed. The third experiment was carried out using all three schemes for different transmission rates. Their results showed that peer-to-peer schemes were better at maintaining position coherency than the client server model. An increase in delay time increased both the RMS position error and the peak position error for all schemes. The force values presented to the user also increased with a decrease in the packet transmission rate. In [24], the authors compared the performance of the virtual coupling schemes implemented on a NIST Net network emulator. This emulation was carried out using delay times experienced in [23] between Seattle, Washington, USA and Italy. The results showed that the performance of the emulator depends on the transmission rate, where high values of transmission rates cause deviation from the results obtained in [23].

In their paper, Bianchini, et. al.,[25] used Linear Matrix Inequality (LMI) to provide a framework for stability analysis and virtual coupling design for multi-contact haptic systems. The LMI approach allowed for taking into account the structural constraints that arise in a multi-contact scenario. As the system may be physically distributed, the virtual coupling, which is often lumped together with the device, may share only limited information with the device and the virtual environment due to decentralization and limited communication requirements. The authors proposed a design procedure for virtual coupling for such a system which was two-fold: first, the levels of passivity to be displayed for guaranteed stability by the virtual coupling and the device are computed, and then the structure of the virtual coupling reflecting the constraints imposed on the system is implemented in a way that allows the effects of the constraints on the realism of interaction can be qualitatively evaluated and tuned. In [26], the authors carried out experiments considering two cases, one where a single operator is using two haptic devices and another where two operators are operating two devices. When a perturbation is present in the environment, the virtual coupling failed to provide stability in the first case, but was successful in the second case. In [27], they expanded their experiments to consider M 1-DOF users not only distributed but also oriented differently. They proposed a class of virtual couplers to stabilize the system which could be parametrized using a sequence of LMI problems and was flexible enough to take into account the decentralization of the users. Using parameters similar to [26], the proposed controller was able to stabilize the system with a non-zero solution.

Šurdilović and Radojićić designed a robust control system to synthesize virtual coupling for haptic interfaces interacting with a virtual environment in [28], which is an expansion of the control theory developed for robot/environment interaction. The performance of the controller was demonstrated on a SISO admittance display. Experiments showed that the interaction of the haptic device with virtual environment was stable, reaching both contact transition stability and coupled stability. The authors carried out experiments showing that a single set parameters for the virtual coupling results in a controller that is robust enough for a wide range of stiffness values for the environment.

In order to improve transparency while maintaining stability in a haptic system with virtual coupling, Zhu, et.al., in [29] attempted to find an equilibrium point between stability and transparency by using the speed gain, position gain and the damping and the mass of the virtual coupling to optimize the loop gains and the virtual coupling impedance. This resulted in a low-inertia high bandwidth haptic interface device which had guaranteed stability and good transparency.

1.3.2 Design of Haptic Devices

A haptic interface is a device that uses mechanical actuators to reflect force back to the user allowing him to touch, feel or manipulate a virtual environment. Adelstein and Rosen [30] designed a two degree of freedom force reflecting manipulandum based on a 5R spherical closed chain linkage joining the output of two DC motors to a handle operated by a user. The motivation of their design was to study the effect of tremor on a human operator. In order to do so, the designed manipulator had an effective operating bandwidth of 12Hz, with various measures to minimize the manipulator's phase lag, which included both mechanical techniques and measures to reduce computational complexities. Their system's potential use include study of psychophysical effects and kinaesthetic interfaces to virtual environment and teleoperation.

Akahane, et. al., [31] designed a high definition haptic controller that was able to render a haptic interaction at 5kHz, using a SuperH4 processor designed by Hitachi Semiconductor. Such a high rendering frequency allows for a higher stiffness of virtual wall to be rendered stably.

An and Kwon [32] proposed a hybrid haptic interface comprising of an active motor and a passive magnetorheological (MR) brake that is controllable. A theoretical study based on passivity and Z-width was carried out to show that the hybrid system was superior to an active interface. The authors also presented a set of experimental results that validated their theoretical deductions. Kwon and Song [33] also designed a hybrid haptic system comprised of both motors and brakes, as motors and brakes can act complimentary to each other. The performance of the hybrid system was compared to an active system composed of motors and a passive system composed of Passivity observers/Passivity controllers (PO/PC). Their experiments showed that their hybrid device is capable of producing a good contact with virtual environments, but suffered from large error in the steady state.

Bullion and Gurocak [34] developed a compact and lightweight haptic glove composed of three MR brakes for actuating the index and middle fingers, as well as the thumb. The authors carried out experiments to verify the force model of the glove. The simplicity of their design was that it removed the need for an additional actuator box.

1.3.3 Virtual Environments and Haptic Systems

Colgate and Brown [35] analysed the effect of different factors on the Z-width of a haptic display. They carried out experiments using a one degree-of-freedom haptic device under sixteen different combinations of the following factors: presence of physical damper, sampling rate, encoder resolution and use of velocity filter. Their results showed that the presence of a physical damper increases both the maximum damping and maximum stiffness. Large values of update rate were shown to increase the achievable level of stiffness, but lowering the damping coefficient. This negative effect can be offset simply by using a digital filter to smooth out the velocity signal. The test subjects also reported that a higher encoder resolution provided a better feel. From these results, the authors concluded that in order to achieve high impedances to provide a more realistic feel of the interaction with a virtual environment, the inherent damping, sensor resolution and sampling rate have to be maximized, while a velocity signal filter should be used to improve the user impression of the wall quality.

Hannford and Ryu [36] designed a passivity observer/passivity controller method for operation with an Excalibur haptic interface with both impedance and admittance causality. The authors carried out a detailed mathematical analysis for the passivity observer and passivity controller. Their design of the controller took into account both series and parallel configurations. They also carried out simulations based on different operating conditions. When in contact with an environment with a high stiffness, the controller improved performance of the haptic device by making the contact bounces passive. When a limit is imposed on how much force could be dissipated by the controller, the performance remained almost the same. Probably one of their most important result was obtained for delayed environments. The passivity controller in this case was able to stabilize very quickly a system that was totally unstable without it.

Abbott and Okamura [37] determined an explicit upper bound on stiffness of virtual walls that is necessary and sufficient for passivity. Their work established the importance of the relationship between the friction and sampling rate, and between the Coulomb friction and the encoder resolution on the upper bound on stiffness while indicating a lack of coupling between the two sets of parameters. The authors carried out a set of experiments under different working conditions based on user force and velocity of the haptic display to verify their findings.

In [38], the authors designed a method of superimposing event-based high frequency transient forces over traditional position-based feedback in order to improve the realism of interactions with virtual environments. When hand-tuned pulses and decaying sinusoids are scaled by impact velocity, they can recreate a realistic interaction. The authors proposed a new method of generating the appropriate transients by inverting the model of the haptic device, which they then used to calculate the force required to create an acceleration profile at the user's end, which was pre-recorded. This approach showed promise as a better way to render a real interaction with a virtual wall than position feedback.

In [39], the authors proposed adaptive nonlinear control schemes for haptic systems with both impedance and admittance type virtual environments. The controllers proposed by the authors does not require any knowledge about the models of the haptic interface, user and the environment. The controllers could alter the dynamics of the haptic device using measurements of user force and velocity, thereby making them suitable for use in high force-large workspace interfaces. Discrete time low-pass filtering was used to substantially decrease the lower bound of the perceived inertia that can be stably represented. Experiments were carried out for both admittance type and impedance type environments. For admittance type environments, the proposed controller had a better performance than a conventional spring damper controller, being able to stably represent higher impedances. On the downside, the adaptive controllers were expensive due to the use of force sensors and the user had to hold the haptic device by the force sensor for proper operation of the controller.

1.3.4 Haptic Systems with Time Delay

In their paper, Wang, et. al., [40] addressed the effect of time delay on haptic operations over a network with time delays. They carried out two sets of experiments with two different haptic devices. One of the experiments was concerned with analysing the effects of delay and noise on the performance of the haptic display. The results showed that the presence of these two factors degraded the performance of the system. The second experiment dealt with the interaction between two identical haptic displays over an Internet link with variable delay. The results show that such a haptic display is unstable, but with application of a compensation technique for the delay, the performance can be improved.

Kim, et. al., [41] in their paper carried out a simple experiment with two users separated by a large physical distance to study the effect of haptic feedback on the performance of the users. They used two Phantom Desktop devices, located on either side of the Atlantic Ocean. Using the Internet2 network and a multi-threaded application where the haptic subsystem ran concurrently with the graphical component, the users were asked to lift a cube rendered in virtual environment with each user using a single probe and working in cooperation with each other. The software component transmitted force rather than position information. The workstation at each end generated an implementation of virtual environment and also showed the presence of the other user. A questionnaire was prepared by the authors that asked how well any one of the users could sense the presence of the other. The answers of this and other questions were quantified in order to get a better idea of the success of a trans-Atlantic haptic cooperative task over the Internet. The approaches taken by the authors in implementing the software environment and also the communication link resulted in each user successfully sensing the presence of the other user and interacting with him.

To improve the performance of a tele-mentoring system in the presence of time delay, Zhou, et. al., [42] proposed a predictive system, where a combination of Kalman and adaptive filters predict the behaviour of the human arm trajectory. The predicted data was used for further processing without buffering based on an estimation of the network delay. The authors also suggested the use of Cartesian space in order to predict human movement.

In their paper, Hulin, et. al., [43] carried out a stability analysis of a haptic system, where the haptic device was colliding against a virtual wall and interacted with a human arm. The authors modelled the wall as a time-delayed discrete-time spring-damper system, while the human arm was modelled as a linear mass-spring-damper system. The linear stability condition derived by them was shown to be unaffected by human arm stiffness, when compared to the influence of the mass of the human arm.

Ferrari and Hu [44] carried out an experiment were they studied the effect of incongruent delay in visual and haptic data in a networked haptic virtual environment. Results from their experiments showed that the guided user in their setup experienced a mismatch in the stiffness of the virtual as the delay between the haptic data and the visual stream reached a value between 66.6 ms and 133.3 ms. Cooper, et. al., [45] designed a simple experiment involving a bimanual pick and place task with incongruent haptic and visual feedback. Their experiments showed that delay in completion of the specified task and mistakes in completing the task were significantly greater when delay was added to the haptic feedback.

1.3.5 Wave Variables and Haptics

Diolaiti and Niemeyer took advantage of the fact that motor inductance can provide a higher stiffness than that achieved by a digital control loop in their paper [46]. This high value of stiffness is evident at higher frequencies. The authors designed analog circuits to take advantage of this fact over a wide range of frequencies. This circuit was described in terms of wave variables, making the external digital loop insensitive to servo delays. Application of wave haptics in conjunction with a proportional controller reduced the high stiffness region to frequencies lower than that for classical approach. Experiments showed higher values of proportional gain improved both the compression and restitution values of the torque and also the rendered stiffness. The approach of wave haptics also made better use of the physical properties of a haptic device which did not require assumption on the mechanical friction for stability and passivity. The use of wave variables also guaranteed robustness to servo delay.

An extension of the wave variable method was performed by Alise, et. al. [47] to include multiple DOF systems. In order to achieve this, the authors designed a family of scaling matrices and orthogonal matrices. By applying the combination of a fixed scaling matrix and any orthogonal matrix, the authors were able to show that only the wave variables are changed, but not the system output, regardless of the delay. Experiments carried out using a Phantom$^{\text{TM}}$ Omni haptic device showed that when implemented in a teleoperation system, the proposed multiple DOF wave variables allowed the slave to track the master in the presence of delay.

When wave variables are employed for teleoperator robotic systems, a bias term deteriorates the haptic performance. Ye and Liu [48] used a augmenting path to add a correction term on the returning wave path at the master side to reduce the effect of the bias term. A low-pass filter on the path removes the extra energy inserted due to the added path in order to maintain passivity. As the bias term is transient, manipulation of this part does not affect the performance in the steady state case.

Alise et.al., [49] devised a method to make the wave variables technique applicable to multiple degrees of freedom, by using scaling matrices. The authors established the necessary conditions to guarantee passivity. Results of experiments carried out by the authors showed that certain classes of matrices improved the performance, while others did not, impacting on how human users used a teleoperation system.

Yasrebi and Constantinescu [50] carried out an analysis using the Jury-Marden stability criterion that showed the one step computational delay introduced when a haptic device interacts with a virtual environment through a wave variable controller, injects energy in the feedback loop, thereby shrinking the stability region of the haptic interaction. Using a time domain passivity analysis, the amount of generated energy was determined. A simple algorithm where the wave variable on the virtual environment side was adjusted based on the value of generated energy, was proposed to compensate for this extra energy. The authors were able to double the z-width of a Phantom Omni interface in experiments carried out using their proposed algorithm.

1.3.6 Projection Based Force Reflection Algorithm

While the force feedback allows human operators to feel interaction with the remote environment, however, in the presence of communication delays the force feedback may destabilize the system. Polushin, et. al., [51] presented a new force reflection algorithm where the reflected force was altered based on the estimate of the human force. Such an alteration is not felt by the human operator, however, it solves the instability issues; in particular, this algorithm allows for the use of a lower damping and higher force reflection gain than can be achieved using conventional methods. While it is assumed in [51] that the human force is directly measured, in [52] the authors use a high gain force observer to estimate the force. The authors have also shown that their proposed algorithm can remove the constraints imposed on the subsystems by the small gain theorem, thereby allowing the use of such an approach in teleoperator systems [53]. A further improvement on the force reflection algorithm was presented in [54]. The authors imposed restrictions on the direction and magnitude of the reflected force which, although is not felt by the user, cancels out the unintentional motion of the master. Such restrictions do not result in stability and/or transparency deterioration. Experimental results based on the projection based force reflection algorithm were presented in [55]. The use of this algorithm significantly increased the admissible force reflection gain without sacrificing stability; the improvement is particularly significant in the presence of communication constraints.

Projection based force reflection algorithm was used to design a cooperative teleoperator system in [56] where the authors defined explicit assumptions on the human dynamics rather than assuming that the user to be an external source of uniformly bounded energy. The authors chose this approach because it eliminates the reliance of stability on the user. With the use of the projection based force reflection algorithm, the authors were also able to eliminate the conservativeness of the small gain approach. Experiments were carried out to show that the projection based force reflection algorithm could provide stable telemanipulation for lower values of interaction forces. This was shown to be true also for the case when the user released the master. The authors were also able to show that in the steady state, the transparency of the system was also very high.

1.4 Objectives of the Thesis

The main objectives of this work are as follows:

1) To implement a virtual environment (virtual wall), which will be used for experimental comparison of different force reflection schemes for haptic interaction.

2) To compare the performance of the Projection-based Force Reflection Algorithm (PFRA) with that of the Virtual Coupling (VC) and Direct Force Reflection (DFR) for a non-delayed haptic system.

3) To compare the performance of the Projection based Force Reflection Algorithm (PFRA) with the Direct Force Reflection (DFR) and Wave Variable (WV) techniques for a haptic system in the presence of time delays.

1.5 Contributions of the Thesis

The major contributions of this work can be listed as follows:

1) The performance of PFRA has been experimentally compared with the performance of VC, WV and DFR. It was shown that the PFRA performed better than the DFR in all test situations, while it was comparable or better than the other two techniques.

2) In terms of the time required to stabilize the end effector of the haptic device, the PFRA was shown to perform the best among the algorithms compared in all test situations.

3) Under the test environment, the PFRA has been shown to be perfectly transparent, allowing it to represent the properties of the virtual environment accurately.

1.6 Outline of the Thesis

The thesis is arranged in the following manner. **Chapter 1** provides a basic overview of haptic systems and brief overview of the work that has been done in the field of haptics and its stability. In **Chapter 2**, issues related to the haptic system and its stability are presented, with a description of the techniques used to maintain stability. The problem dealt with in this work is described in **Chapter 3**, along with description of the equations used. The results of the different experiments carried out are presented in **Chapter 4** and **Chapter 5**, while conclusions based on these results are presented in **Chapter 6**.

Chapter 2

Haptic Systems: Stability Issues

2.1 Introduction

Haptic devices and their stability issues are usually studied in relation to interactions with a virtual environment. In this chapter, the virtual wall is discussed in brief, particularly the concept of passivity of the virtual wall. The notion of Z-width, which is an important performance characteristic of a haptic system, is also discussed. Techniques for improving stability of both non-delayed and delayed haptic systems, including virtual coupling, wave variables, and projection based reflection algorithms, are also elaborated here.

2.2 Virtual Walls

A virtual wall, whose implementations can vary according to hardware and software details, is the standard haptic task. Since any virtual environment can ultimately be reduced to a combination of virtual walls, all interactions with such environments can be reduced to interactions with virtual walls of varying stiffness and damping. As a result, a virtual wall is frequently used as a benchmark for haptic interfaces [4].

The most common approach to implement a virtual wall requires a back drivable manipulandum and a discrete time controller [57]. If $x(t)$ is the position of the manipulandum end-effector, let x_k and $\dot{x}_k$ denote the sampled versions of the end-effector position and velocity, respectively. If the position of the manipulandum x_k is inside the wall, an interaction force F_k is generated according to the formula

$$F_k = \begin{cases} K(x_k - x_{wall}) - B\dot{x}_k & x \geq x_{wall}, \\ 0 & x_k < x_{wall}, \end{cases} \tag{2.1}$$

where x_{wall} is the position of the wall, $K \geq 0$ is a virtual stiffness and $B \geq 0$ is a virtual damping coefficients. The force F_k is transformed into the analog form $F(t)$ and consequently applied to the actuators of the haptic device. Note that the formula (2.1) is not the

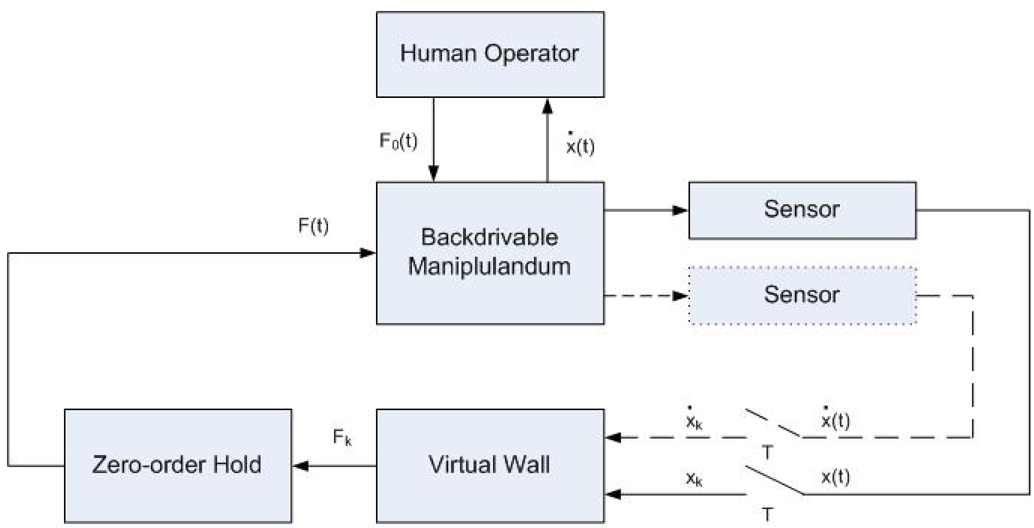

Figure 2.1: Block Diagram of a common implementation of the Virtual Wall [57]

only possible way to realize a virtual wall; for instance, nonlinear characteristics of the virtual wall's impedance may be implemented in the software. Also, the sensor that measures the end-effector velocity can be replaced with an estimator, which can be used to derive the velocity information from the position measurements.

2.2.1 Passivity of Virtual Walls

When interacting with a virtual wall using a haptic device, the user should experience a feeling of interaction similar to the one with a real wall. However, since a haptic device is a sampled data system combining a continuous time mechanical system with a discrete time controller, the effect of sampling may cause the haptic display to lose passivity. As a general rule, there is always some penetration into the virtual wall by the haptic device [4]. When the controller detects the wall penetration, the environment will compute a large output force normal to the surface of the wall at the next sampling interval. As a result, the haptic display will be pushed outside of the wall rapidly. At a future sampling interval, the environment will detect that the haptic display is no longer in contact with the virtual wall and the force acting on the display will become zero. When this sequence of events (haptic device in and out of contact with the wall) is repeated, it results in oscillations. This destabilizing effect arises because of two factors:

a) The exact time when the haptic display contacts the virtual wall can not be detected due to sampling.

b) The resolution of the position sensor has the effect of quantizing the penetration distance into the wall.

Minsky et. al., [58] proposed a criterion relating different wall parameters to the sampling period T of the digital system to implement a virtual wall that presented a more realistic feel to the user. Their criterion was as follows,

$$\frac{B}{KT} > c \tag{2.2}$$

where c is a constant with a value approximately equal to 0.5. However, the authors obtained this result on the basis of maintaining wall stability. Stability is a system property, and is therefore dependant on operator dynamics as well as wall dynamics. Since the operator dynamics are non-linear and can be changed radically, it is difficult to use stability as a basis of a performance criterion without taking the full range of human dynamics into consideration. In fact, authors in [57] reported that they were unable to reproduce the above result.

The authors in [57] proposed that a better basis for a measure of performance is passivity

- the inability to act as an energy source. If the human-virtual wall interaction results in oscillations, the wall is said to be 'active', or that it acts as a source of energy. This is true because the frequencies involved in the oscillation are often outside the range of voluntary motion (up to 10Hz). Such oscillations are not present in the case of real walls. The fact that virtual walls being active is apparent from the behaviour of a virtual spring. As this spring is implemented in discrete time, the average force during squeezing will be less than the average force during release. As a result, a discrete-time implementation of the spring typically generates energy.

In such a case, the necessary and sufficient conditions for passivity will be given by [4],

$$b > \frac{T}{2}\frac{1}{1-\cos\omega t}\Re\left\{(1-e^{-j\omega t})H(e^{j\omega t})\right\}, \qquad \mathit{for}\, 0 \leq \omega \leq \omega_N \tag{2.3}$$

where, b is the physical damping present in the mechanism, T is the sampling period, $H(z)$ is a pulse transfer function representing the virtual environment [4] and $\omega_N = \frac{\pi}{T}$ is the Nyquist frequency. Colgate and Schenkel [59] assume that the transfer function of the wall is

$$H(z) = K + B\frac{z-1}{Tz}, \tag{2.4}$$

which results in a simplified sufficient condition for passivity, as follows,

$$b > \frac{KT}{2} + |B|. \tag{2.5}$$

The physical damping, therefore, has to be sufficiently large to dissipate the excess of energy generated in the wall in order to maintain passivity.

2.3 *Z*-width

A haptic interface can essentially be thought of as a device that generates mechanical impedance, which represents a dynamic relationship between velocity and force. In the real world, such impedances may have an extremely wide range. Movement in free space can be represented by zero impedance, while the contact with a rigid object should be represented by a very high (ideally, infinite) impedance. Ideally, a haptic device should be able to generate impedances at both extremes. The focus in designing practical haptic devices is to create a system that can exhibit a broad dynamic range of impedances. This dynamic range of impedances is defined as the Z-width of the haptic device [4]. This is essentially the difference between the maximum and minimum impedances that can be rendered [6],

$$Z_{width} = Z_{max} - Z_{min} \tag{2.6}$$

A haptic device with a large Z-width will be able to render a more realistic virtual environment. This term is a measure of the potential of the haptic device, and can be used as a parameter of comparison of different device.

The lower bound of the Z-width is usually bound by the overall mechanical design. The upper bound of this impedance is usually determined by the computational capabilities of the system. Some approaches for increasing the maximum impedance that can be rendered by a haptic device are as follows [35]:

a) Increasing physical damping;

b) Increasing sensor resolution;

c) Increasing sampling rate;

d) Filtering the velocity signal.

While maintaining passivity is an intuitive approach to increase the Z-width, it also imposes restrictions on virtual environment stiffness and damping. As a result, the focus of research has shifted to increasing the maximum impedance as a way to increase the Z-width.

A virtual wall can be used to characterize the Z-width of the haptic device. The convention of graphically representing Z-width is by using virtual stiffness-virtual damping plots. Since this type of plots do not take into account the effect of frequency on Z-width, a better method of representation can be as a set of curves showing the upper and lower bounds of impedance as a function of frequency, while maintaining passivity.

For practical applications, the maximum impedance, and so the Z-width, can be increased using a variety of methods. For instance, controllers like virtual coupling and passivity observers/controllers, or mechanical or electrical methods can be used to dissipate the excessive energy. In recent times, techniques successful in maintaining stability in teleoperator systems, like wave variables and projection based force reflection algorithm, have received attention.

2.4 Virtual Coupling

The technique of virtual coupling was proposed by Colgate and his colleagues [12] to improve the stability of virtual environments rendered using haptic displays. It is a basic and one of the most popular techniques used to improve the performance of a haptic system. It consists of a virtual spring and virtual damper in mechanical parallel that connect the haptic display to the virtual environment. Virtual coupling simplifies the problem of maintaining stability by making it necessary only to satisfy the following two conditions [4]:

a) Proper selection of virtual coupling parameters;

b) Creation of a discrete time passive virtual environment.

Ensuring that the virtual environment is passive is easier than ensuring that the entire haptic system is passive. Such a conceptual division of components of the haptic system allows the user to consider passivity for each element separately. Proper selection of the virtual coupling parameters allows the maximum environment impedance to be reduced and matched to the passivity limits of the haptic device. While this makes the rendered impedance to be within the Z-width of the haptic display, this range is usually lower than the actual impedance of the virtual environment. This discrepancy in the rendered and

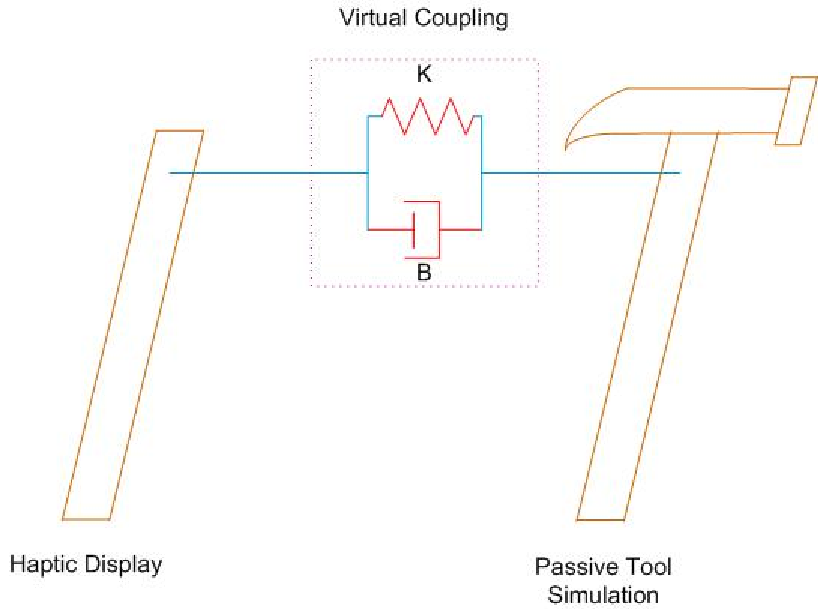

Figure 2.2: Virtual coupling [4]

actual impedance of the virtual environment, or the lack of transparency is the major drawback of the virtual coupling system.

The primary concept of maintaining passivity is to dissipate the excess of energy generated in the system, which may otherwise result in instability. The environment parameter α_e, measuring the lack of passivity, must satisfy the following relationship,

$$\alpha_e < \delta \tag{2.7}$$

where, δ is the physical dissipation in the system. The virtual coupling modifies this equation with its impedance γ, as follows [4]:

$$\alpha_e < \frac{\delta\gamma}{\delta + \gamma}. \tag{2.8}$$

This modification actually allows the virtual environment to generate certain amount of power while be still maintaining passivity of the overall system.

2.5 Wave Variables

Force feedback in teleoperator systems improves the ability of an operator to perform complex tasks, especially when there is an interaction with a remote environment. However, the remoteness of the environment introduces time delay in the system which, if left untreated, may result in instability due to unwanted power generation in the communication link. In order to deal with this problem, damping can be introduced into the system. This solution, however, also suffers from significant drawbacks. Adding extra damping does not necessarily guarantee stability, but designs incorporating this feature limit system performance. To overcome this shortcoming, Niemeyer and Slotine [60] presented a method based on passivity analysis and the concept of wave variables. Wave variables encode the complementary pair of power variables of velocity $\dot{\mathbf{x}}$ and force $\bar{\mathbf{F}}$, according to the following formulas:

$$\mathbf{u} = \frac{b\dot{\mathbf{x}} + \mathbf{F}}{\sqrt{2b}}, \qquad \mathbf{v} = \frac{b\dot{\mathbf{x}} - \mathbf{F}}{\sqrt{2b}} \tag{2.9}$$

The wave variable $\bar{\mathbf{u}}$ is the forward moving wave, from the master to the slave and $\bar{\mathbf{v}}$

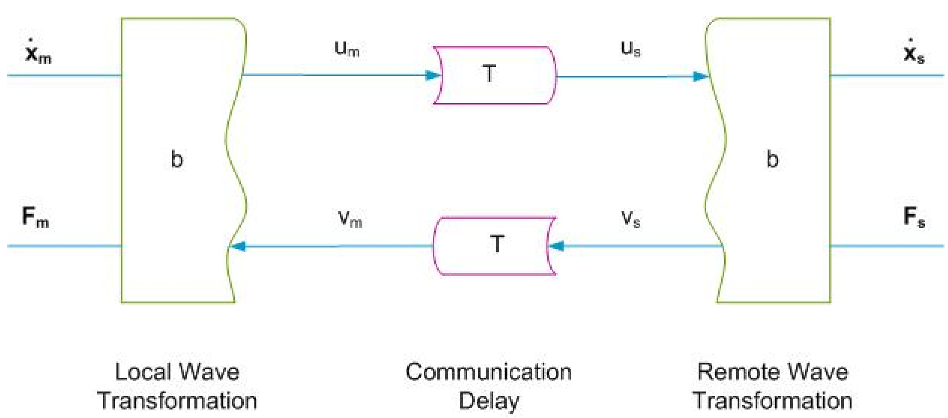

Figure 2.3: Wave variable transformation at local and remote site [61]

is the backward moving wave, going from the slave to the master. A positive constant b is called the characteristic wave impedance; it acts as a tuning parameter matching the controller to a particular task. In the presence of communication delay, the transmission of wave variables instead of the power variables allows to maintain passivity according to the following equation [62]:

$$\int_0^t \frac{1}{2}{u_s}^T u_s + \frac{1}{2}{v_m}^T v_m \, d\tau \leq \int_0^t \frac{1}{2}{u_m}^T u_m + \frac{1}{2}{v_s}^T v_s \, d\tau + E_{store}(0), \qquad \forall t \geq 0. \tag{2.10}$$

The wave transformation (2.3) is bijective; it therefore allows to recover the power variables without loss of any information, according to the following equations

$$\dot{\mathbf{x}} = \frac{1}{\sqrt{2b}}(\mathbf{u} + \mathbf{v}), \qquad \mathbf{F} = \sqrt{\frac{b}{2}}(\mathbf{u} - \mathbf{v}) \tag{2.11}$$

The algebraic loop allows the use of the information in the returning wave variable to

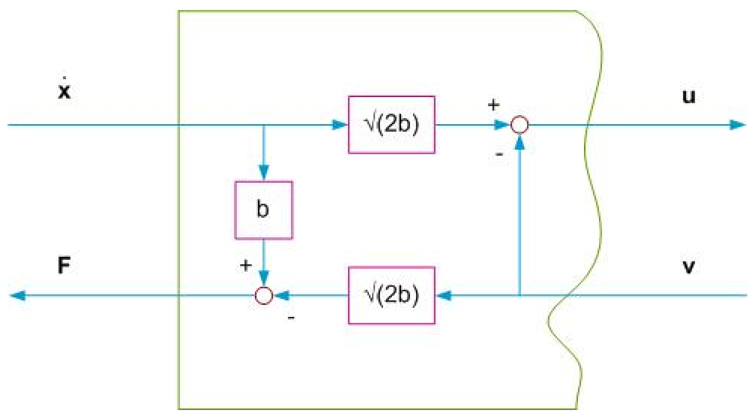

Figure 2.4: Interface between wave variables and power variables [61]

encode the forward going wave variable,

$$\mathbf{u} = -\mathbf{v} + \sqrt{2b}\dot{\mathbf{x}} \tag{2.12}$$

The knowledge of the returning wave can also be used to generate a force feedback command for the master,

$$\mathbf{F} = b\dot{\mathbf{x}} - \sqrt{2b}\mathbf{v} \tag{2.13}$$

In practice, wave transform provides an interface between the signals represented in terms of power and wave variables [61] without loss of information, while maintaining passivity in the presence of time delay.

2.6 Projection Based Force Reflection Algorithms

In bilateral teleoperation, the flow of information is bidirectional: the position and/or the velocity of the master are sent to a remote slave, while the force information is fed back from the slave to the master. While the presence of such a feedback creates kinaesthetic feeling of interaction with the remote environment, the presence of delay in the communication link can also introduce severe restrictions on overall stability and transparency of the system. This problem is more significant when the system comes into contact with a rigid environment. There is subsequently often a trade off between stability and high force reflection gain. A high force reflection gain can provide the user with a stronger haptic feeling of the remote environment, but at the same time increases instability by increasing the closed loop gain [55]. The presence of time delay in the communication link further aggravates this problem as it destroys the natural passivity of the system.

In order to provide a high level of transparency while maintaining overall system stability, Polushin, et. al., [51] proposed a new method known as the Projection Based Force Reflection Algorithms (PFRAs). The idea behind these algorithms is to decompose the reflected force into two components: one that is compensated by the human hand and the other that is not. The human user immediately feels the first component, while the second component is directly responsible for the creation of induced master motion. As this second component is the reason behind instability, the PFRA attenuates it. The force reflected to the motors of the master is defined by the equation [55],

$$f_r = \alpha f_{env} + (1 - \alpha)\phi_{env} \tag{2.14}$$

In Equation 2.14, f_{env} is the force signal that arrives from the slave device directly. ϕ_{env} is generated according to the Equation 2.15 as follows,

$$\phi_{env} = \operatorname*{Sat}_{[0,1]} \left\{ \frac{f_{env}^T f_h}{\max\left\{|f_h|^2, \epsilon_1\right\}} \right\} f_h \tag{2.15}$$

α is a weighting coefficient and is defined as $\alpha \in [0, 1]$, ϵ_1 is a small positive constant, f_h is an estimate of the human force obtained from a force observer, and,

$$\underset{[0,1]}{\mathrm{Sat}}\{x\} = \max\{a, \min\{x, b\}\} \tag{2.16}$$

ϕ_{env} obtained from Equation (2.15) is the component of the reflected force that is compensated by the human hand and is felt by the user. From Equation (2.14), it is clear that ϕ_{env} is fed back to the user with a gain of 1, while $(f_{env} - \phi_{env})$, which is the residual force that is not felt by the user, is attenuated with a gain of $\alpha \in [0, 1]$.

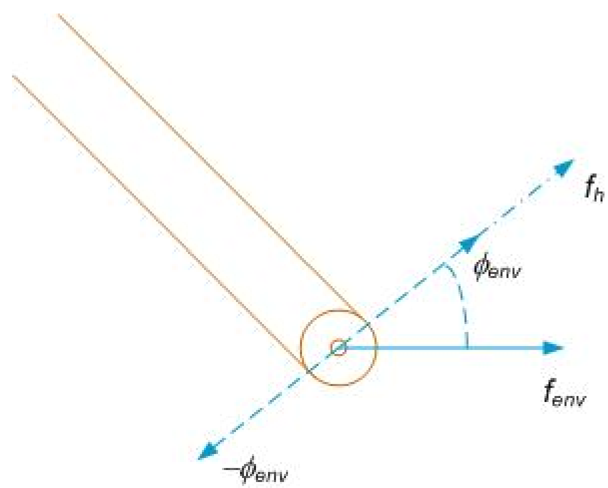

Figure 2.5: Decomposition of reflected forces in the projection-based force reflection algorithms [63]

2.7 Conclusion

This chapter has focused on different issues related to the stable interaction between a haptic device and a virtual environment. Since the virtual wall is an important benchmark in studying the performance of haptic systems, its implementation was described, with particular focus on the concept of passivity of the wall. Z-width, the range of impedances that the haptic device can describe, was also discussed. Finally, different techniques currently in use to increased the z-width and improve the stability of haptic systems, such as virtual coupling, wave variables and projection based force reflection algorithm, have been discussed, with particular attention to the equations required to implement the equations.

Chapter 3

Problem Formulation and Experimental Setup

3.1 Introduction

As stated in Section 2.2.1, the digital nature of implementation of virtual environments, namely the effects of sampling and quantization processes, doesn't allow for easy rendering of a stiff virtual wall. Lack of passivity results in instability when a haptic display comes into contact with a virtual wall. In order to improve stability of the system, various control schemes have been proposed in the literature. Virtual coupling, which is a combination of a spring and a damper, is a popular method to improve stability of haptic systems. This method has been applied to systems where it is assumed that there is no time delay. However, this control method generally sacrifices transparency in order to achieve stability. Niemeyer and Slotine [60] proposed an approach for systems with time delay which is based on wave variables; however, they applied this method only to teleoperator systems and not to haptic systems. An extension of wave variables to haptic systems was presented by Yasrebi and Constantinescu in [50]. Like the virtual coupling method, though, this technique only addressed the stability issue, without paying attention to transparency. The projection-based force reflection algorithm (PFRA) has been applied by Polushin, et.

al. [52] to teleoperator systems without loss of either transparency or stability. However, this technique has not been applied yet to haptic systems for interaction with virtual environments.

This thesis deals with experimental investigation of the projection-based force reflection algorithms for haptic interaction with virtual environments. In particular, these algorithms are experimentally compared to more conventional techniques known from the literature in terms of their stability and transparency properties, for the case without communication delays as well as in the presence of communication delays between the haptic device and the virtual environment. The main question addressed in this thesis can be formulated as follows: do the projection-based force reflection algorithms provide improvement in stability and transparency properties of the haptic displays for interaction with virtual environments, in comparison with the existing methods? The thesis presents results of a detailed experimental investigation that answer the above formulated question. Below, the experimental setup and the methodology of the experiments are described in some detail.

3.2 Experimental Setup

In order to carry out the experiments necessary to find out the applicability of PFRA in haptic systems, a suitable virtual environment was needed. The virtual wall was chosen for this purpose because of its use as a benchmark in analyzing haptic displays. It was implemented following the technique presented in [57] and described in Equation (2.1). The interaction was modelled as a 1-DOF interaction, with movement of the end-effector in only the x-direction. This model allowed a simple implementation of a haptic system, while at the same time reducing the effect of unwanted movement along the other two axes.

The setup used for the experiments is shown in Figure 3.1. A PHANToM Omni from SensAble Technologies Inc. was the device of choice in the experiments. It is a 6-DOF pen-based master, which was interfaced with an IBM-PC through a Firewire port. The PC

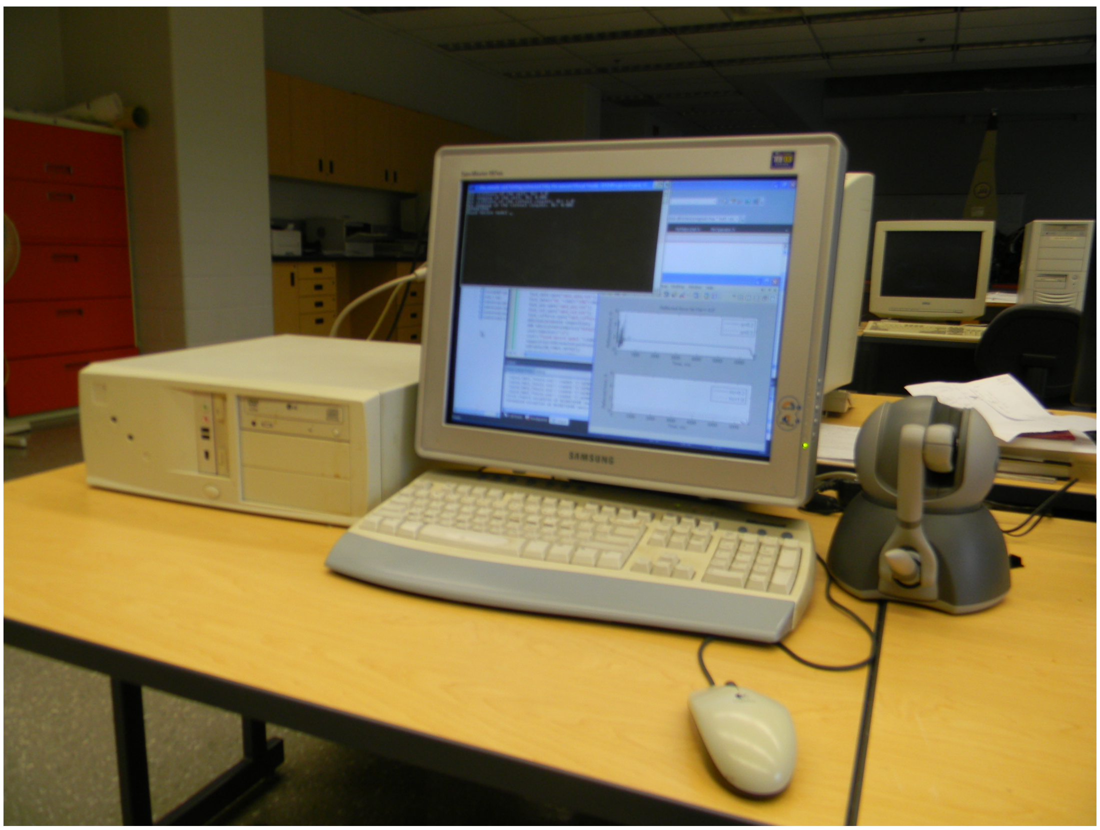

Figure 3.1: Experimental Setup

used a Intel® Pentium®4 processor operating at 2.60 GHz, and 1GB of RAM. With the aid of OpenHaptics Toolkit, based on Microsoft Visual C++, all programs for the virtual wall, virtual coupling, wave variables and PFRA were implemented.

At the beginning of each set of experiments, the different variables describing the techniques and the virtual wall was chosen, the operator was asked to grasp the end-effector of the haptic device and push against the virtual wall, taking care to move the device along the x-axis only. The operator attempted to move the end-effector in the same way during each iteration of the experiment. Each set of variables was repeated several times to ensure reproducibility and eliminate accidental mistakes. Also the operator took a break every 3 or 4 iterations to prevent fatigue and prevent the device motors from overheating. At the same time, the device was recalibrated to eliminate the chance of mechanical errors. Upon obtaining data for each iteration, they were saved for future analysis. The human hand can generate commands with frequencies ranging from 0 Hz to 10 Hz, typically biased towards the lower end of the spectrum, but is able to distinguish forces and vibrations up to 1 khz [62]. In our experiments, a high gain observer is used in order to estimate the human force; the observer is described in Appendix B. As the human force estimate may have high frequency components which cannot be generated by the human hand, a low pass filter with a cut-off frequency of 31.4 rad/s (or 10 Hz) is used on the human force estimate to eliminate the presence of undesired vibrations.

3.3 Virtual Coupling

Both the virtual wall and the virtual coupling are defined by spring-damper systems. Under the combined effect of these two spring-damper system, the proxy position (or the avatar) of the end-effector of the device will be given by,

$$\begin{aligned} p_{new} =& p_{old} + T \times (\frac{1}{(B_c + B_w)} \times (K_c \times p_{dev}) + (K_w \times p_{wall}) \\ &+ (B_c \times v_{dev}) - p_{old} \times (K_c + K_w)) \end{aligned} \tag{3.1}$$

and the velocity of the wall will be calculated using a dirty derivative filter. Finally, the force is calculated as,

$$f = -K_w \times (p_{old} - p_{wall}) - B_w \times v_{wall} \tag{3.2}$$

In the above equations, the following notations have been used,

p_{new}=new position of the wall

p_{old}=old position of the wall

T=sampling interval

B_c = damping of the virtual coupling

B_w = damping of the virtual wall

K_c = stiffness of the virtual coupling

K_w = stiffness of the virtual wall

p_{dev} = position of the end effector

p_{wall} = initial position of the wall

v_{dev} = velocity of the end effector

v_{wall} = velocity of the virtual wall

f= reflected force

A flowchart of the operation of the virtual coupling technique is shown in Figure 3.2.

3.4 Wave Variables

The wave variable technique attempts to overcome the instability issues in teleoperator systems with time delay. This technique has been implemented by Yasrebi and Constantinescu [50] for haptic systems. The technique has shown promise in overcoming the effects of delay, but is also susceptible to proper selection of the parameter b.

On the master side, the wave variable u_m is calculated from the wave variable v_m and the velocity of the device as follows,

$$u_m = -v_m + \sqrt{2b}\dot{x} \tag{3.3}$$

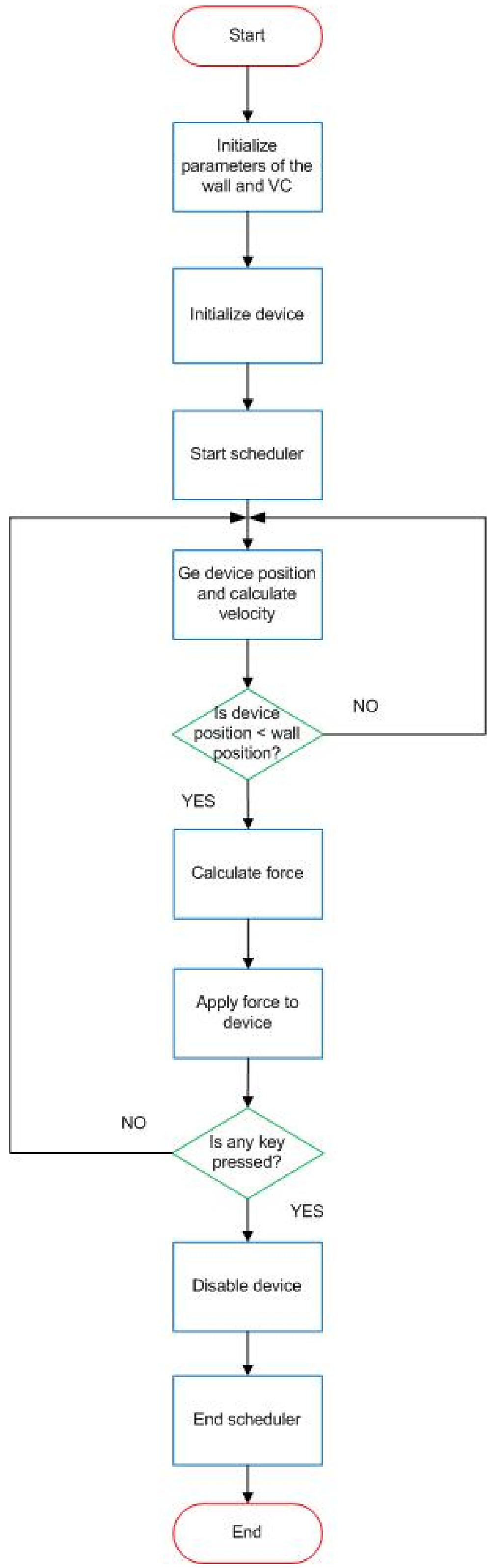

Figure 3.2: Flowchart of Virtual Coupling Technique

The velocity of the slave device is obtained from the following equation, where u_s is the version of u_m on the slave side.

$$\dot{x} = \sqrt{\frac{2}{b}}u_s - \frac{F_s}{b} \tag{3.4}$$

The position information obtained from this velocity information, is used to calculate the contact force F_s according to the eq.-2.1. This contact force is then used to determine the value of the wave variable v_s as follows,

$$v_s = u_s - \sqrt{\frac{2}{b}}F_s \tag{3.5}$$

After appropriate delay, the value of v_m, which is the delayed version of v_s on the master side, is used to calculate the value of the reflected force,

$$F_m = b\dot{x} - \sqrt{2b}v_m \tag{3.6}$$

This force is then applied to the haptic device. The flowchart of operations for the wave variables technique is shown in Figure 3.3.

3.5 Impedance Matching

The haptic device is operating under force control where the returning wave variable v_m is used to generate a force command F_m and applied to the device. Such a force controller can not be perfectly impedance matched. Adding a damping element, D helps reduce the reflections. The combined in that case will be,

$$\frac{F_m(s)}{sX_m(s)} = m_m s + D \tag{3.7}$$

Although no value of D can eliminate the reflection term, choosing $D = b$ [1] allows the two frequency component to be minimized. One drawback to this system is that the high frequency component will remain.

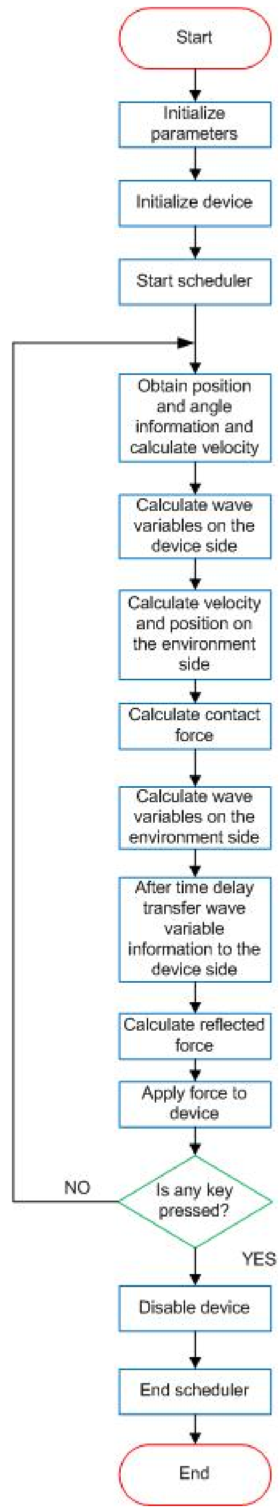

Figure 3.3: Flowchart of Wave Variables Technique

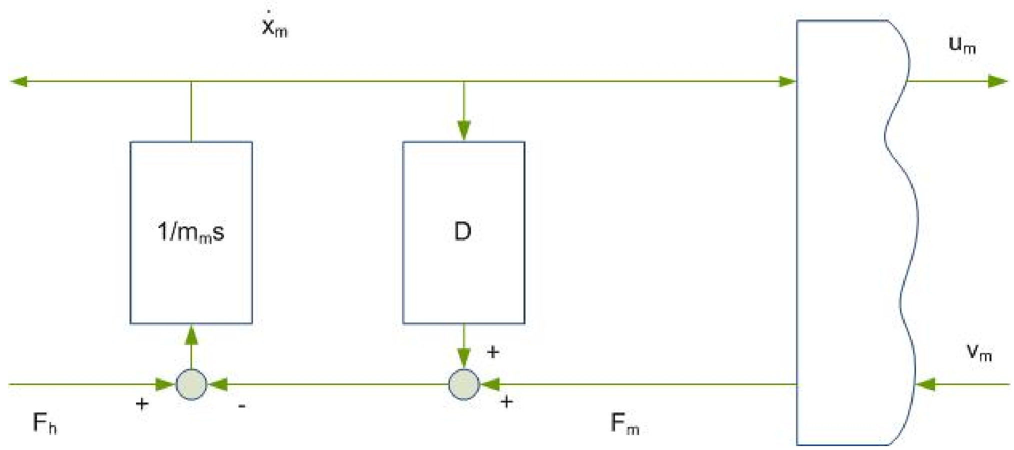

Figure 3.4: Impedance Matching Technique [1]

3.6 Projection based Force Reflection Algorithm

The projection based force reflection algorithm has been shown to be successful in improving the stability of teleoperator systems [52, 53, 55], without sacrificing transparency. This technique allows the component of the contact force that is compensated by the human force to greatly influence the force reflected to the haptic device as described in Section 2.6. The advantage of this is that the uncompensated portion of the contact force, the source of unwanted oscillations would be suppressed and hence have only minor influence on the final reflected force.

Upon obtaining information from the haptic device regarding position and angle, the contact force is calculated according to equations described in Section 2.6. Using a model of the haptic device and the high gain observer, which is described in the Appendix B, an estimate of the human force is obtained. This force is used to determine the component of the contact force that is compensated by the human force according to equation-2.15, which is reproduced here,

$$\phi_{env} = \underset{[0,1]}{\mathrm{Sat}} \left\{ \frac{f_{env}^T f_h}{\max\left\{|f_h|^2, \epsilon_1\right\}} \right\} f_h \tag{3.8}$$

This force is then used to calculate the reflected force as,

$$f_r = \alpha f_{env} + (1 - \alpha)\phi_{env} \tag{3.9}$$

Proper selection of the parameter $\alpha \in [0, 1]$ is important as it determines the amount of influence the component ϕ_{env} will have on the final reflected force, which is fed back to the haptic device. The flowchart for the operation of the projection-based force reflection algorithm is shown in Figure 3.5.

3.7 Apparent Stiffness

Whenever there is interaction between a haptic device and a virtual environment, a force is generated according to equation-2.1 and applied back to the haptic device. This force, as seen from the equation dependent on the stiffness K_w and damping B_w of the wall. However, when a stable condition of the system is reached, represented by the stationary position of the device, the velocity of the device is zero, nullifying the effect of damping on the reflected force, leaving only the force determined by the stiffness. As a result, a measure of the stiffness of the wall may be obtained from the ratio of the reflected force and penetration into the wall by the haptic device.

$$K_{w_{app}} = \frac{F_r}{x_{dev}} \tag{3.10}$$

This measure of stiffness is used as a yardstick to compare the transparency of the different techniques. As this apparent stiffness is measured at the stable state for all the techniques, this gives a good indication of the stiffness of the virtual wall that the user feels.

3.8 Conclusion

In this chapter, the problem addressed in this thesis has been formulated. The experimental setup has been described together with the methodology of the experiments. The three techniques: virtual coupling, wave variables and projection based force reflection algorithm

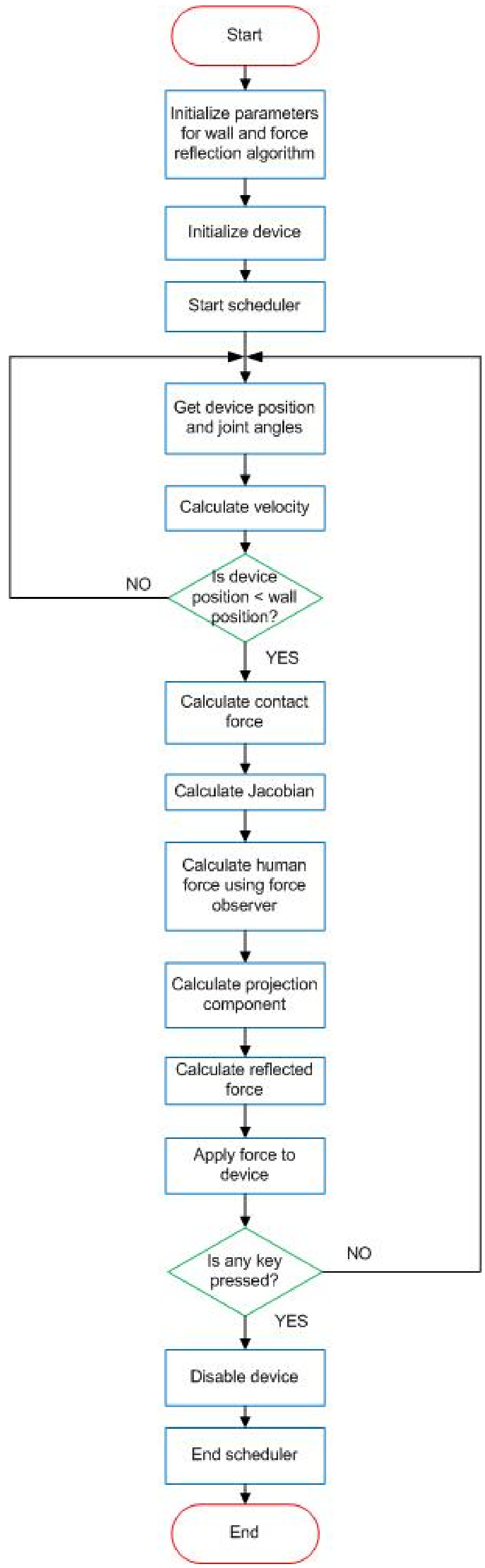

Figure 3.5: Flowchart of Force Reflection Technique

were discussed; in particular, the exact equations used to calculate the forces generated during the interaction were presented. Additionally, flowcharts for the three techniques used were shown. Finally, apparent stiffness is defined as the measure used for comparing the transparency of the three techniques.

Chapter 4

Haptic Interaction without Communication Delays

4.1 Introduction

The first set of experiments were conducted with the purpose of comparing the performance of virtual coupling (VC), direct force reflection (DFR) and projection-based force reflection algorithm (PFRA), in the case where there is no communication delay between the haptic device and the virtual environment. The parameters used as a basis for comparison of stability were different wall stiffness and update rates. In order to find out the transparency of the system, apparent stiffness is used as a measure. Finally the performance of the PFRA was studied based on the value of the weighting coefficient α.

4.2 Experiment 1: Virtual Wall Stiffness

The first experiment was carried out with the purpose of evaluating the stability properties of the three techniques under study when the haptic device is interacting with a virtual wall of varying stiffness. The stiffness of the VC was set at 1.0 N/mm and damping at 0.5 Ns/mm. The damping of the virtual wall was set at 0.005 Ns/mm. The update rate of the reflected force is set at a fixed value of 50 Hz and the response of the techniques were observed for moderate and high levels of stiffness. In the case of PFRA the value of α was fixed at 0.2, while for DFR it is 1.0. For PFRA observations of their behaviour for a moderate value of stiffness, 3 N/mm, are presented in Figure 4.1 in terms of reflected force. From the results presented in the figure, it is apparent that both the VC and PFRA are faster in reaching a stable value of the reflected force than DFR. The amount of oscillation present in the reflected force is comparatively greater for the DFR than both PFRA and VC. PFRA and VC have a similar level of oscillations in this case. However, when the stiffness of the virtual wall is increased to a high value of 10 N/mm, the situation changes, as depicted in Figure 4.2. In this figure, the results show that the PFRA outperforms the other two techniques by a large margin. The performance of the PFRA does not degrade with increased stiffness. However, both the DFR and VC suffer from a severe degradation in performance. This is more significant in the case for VC, which demonstrated a very good response for low values of virtual wall stiffness.

The position information for the three techniques are presented in Figures 4.3 and 4.4. From these figures, PFRA is shown to be better than DFR and VC in terms of reaching a stable position for the end effector of the haptic device. For the lower value of the wall stiffness, it is clear that the PFRA helps the device achieve a stable position the fastest. The VC suffers from initial contact oscillation similar to the PFRA, but requires a far greater amount of time to reach the stable position. While the position of the end effector reaches the final position relatively quickly for the DFR, the initial contact oscillation is greater than the other two cases. For the higher value of stiffness, for which results are presented in Figure 4.4, it is clear that for the case of VC, the end effector penetrates the farthest, presenting a softer than natural feel of wall to user. The oscillations present in the device are also high before it reaches a stable position. For DFR, while it does not penetrate as much as in the case of VC, the end effector suffers from a high level of oscillations. The PFRA provides the best result in this case, where the end effector becomes stable fastest and with the least oscillations.

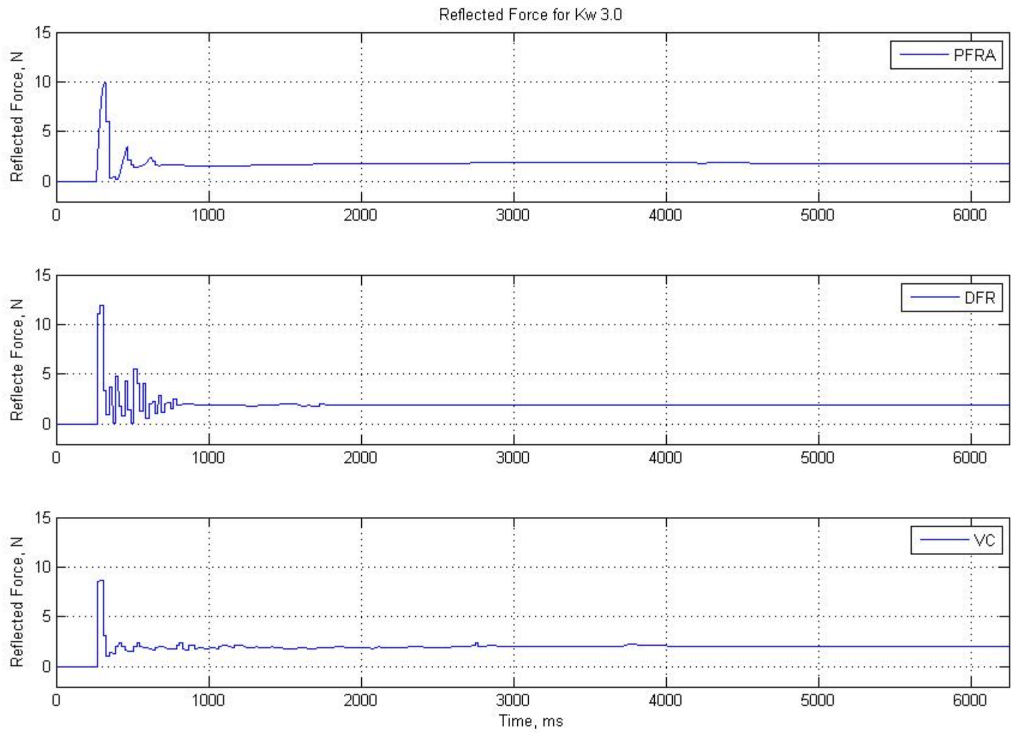

Figure 4.1: Reflected force for $K_w = 3N/mm$

4.3 Experiment 2: Update Rates

As has been stated earlier, it has been shown in [58] that high update rate is desirable for stable operation of the haptic device in contact with a virtual environment. The objective of the second set of experiments was to find out the effect of changing update rate has on the stability performance of a haptic device. The stiffness of the VC was set at 1.0 N/mm and damping at 0.5 Ns/mm. The damping of the virtual wall was set at 0.005 Ns/mm and the stiffness was set at 5.0 N/mm. Two different update rates were used for this experiment: 500 Hz and 50 Hz. The results for PFRA is presented in Figure 4.5 for reflected forces and in Figure 4.6 for the level of penetration by the end effector into the virtual wall. In this case the the value of α was set at 0.2. From Figure 4.5 it can be seen that the initial contact oscillation increases slightly for the PFRA. However, it does not last long. This is further

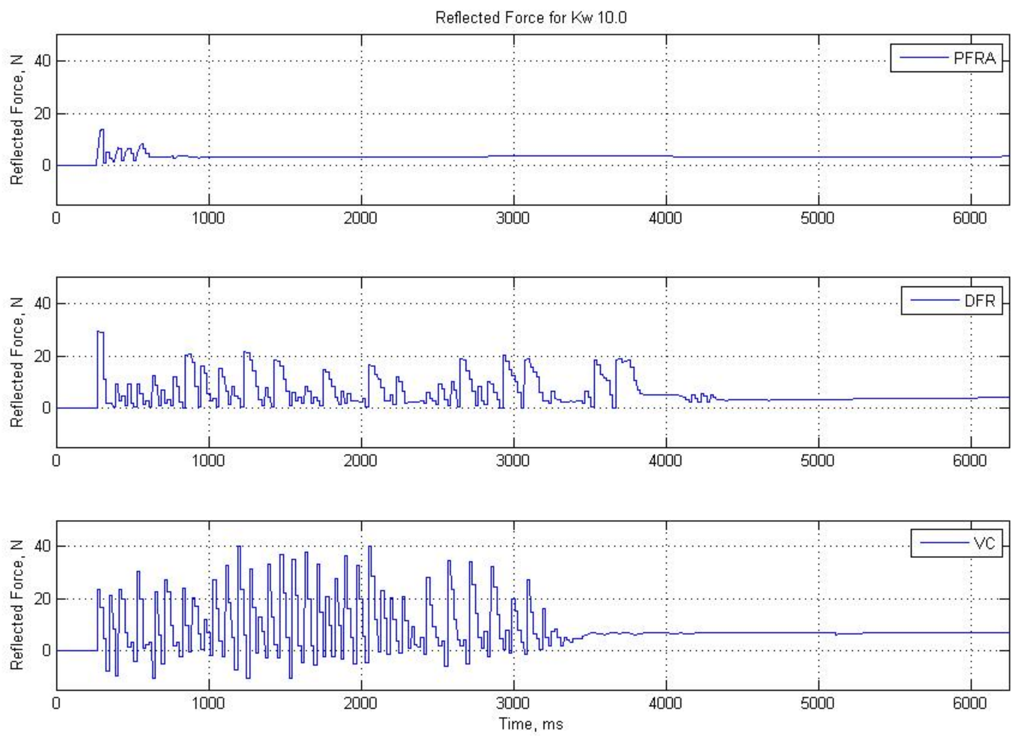

Figure 4.2: Reflected force for $K_w = 10N/mm$

supported by the information presented in Figure 4.6, where the position information of the end effector of the device is presented and shows that the end effector comes to rest at a stable position in a short amount of time.

In Figure 4.7, the results for the reflected force for DFR is presented, where α is set to 1.0. The DFR suffers from severe deterioration in performance as the update rate is lowered. The amount of force oscillations suffered by the DFR increases significantly as the update rate is lowered. This is also apparent from the results presented in Figure 4.8. From the position information presented in this figure, it is clear that the end effector suffers from significantly larger amount of oscillations as the update rate is lowered, which is readily experienced by the user.

The results for VC are presented in Figures 4.9 and 4.10. From Figure 4.9, it can be seen that the reflected force for higher values of the update rate reaches a stable value very

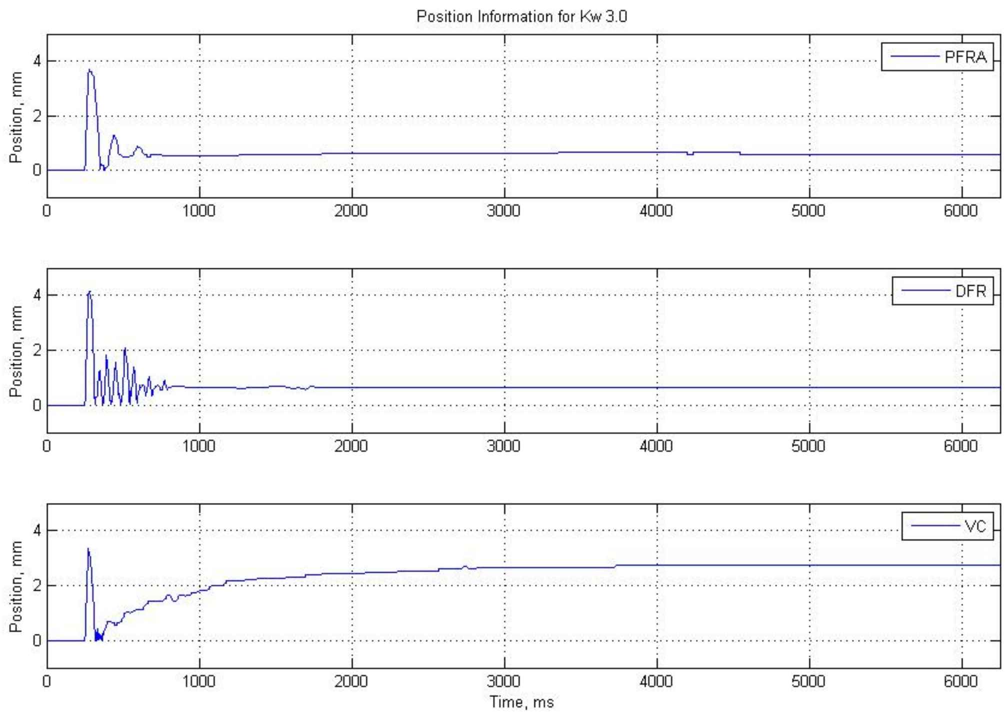

Figure 4.3: Position Information for $K_w = 3N/mm$

quickly, with very little initial contact oscillation. However, VC does not perform as well for lower update rates. Not only does it take longer to come to a stable value, the reflected force also has a higher contact value than for higher update rates. A similar picture is presented in Figure 4.10, where it can be seen from the position information of the end effector of the haptic device that suffers from a larger amount of oscillations due to reduced value of the update rate. Such a change in the level of oscillations is felt by the user and is detrimental to ease of operation of the device.

4.4 Experiment 3: PFRA Parameter α

The performance of the PFRA is dependent on the parameter α. α can have a value between 0 and 1. The value of this parameter determines the relative weight of the components of the

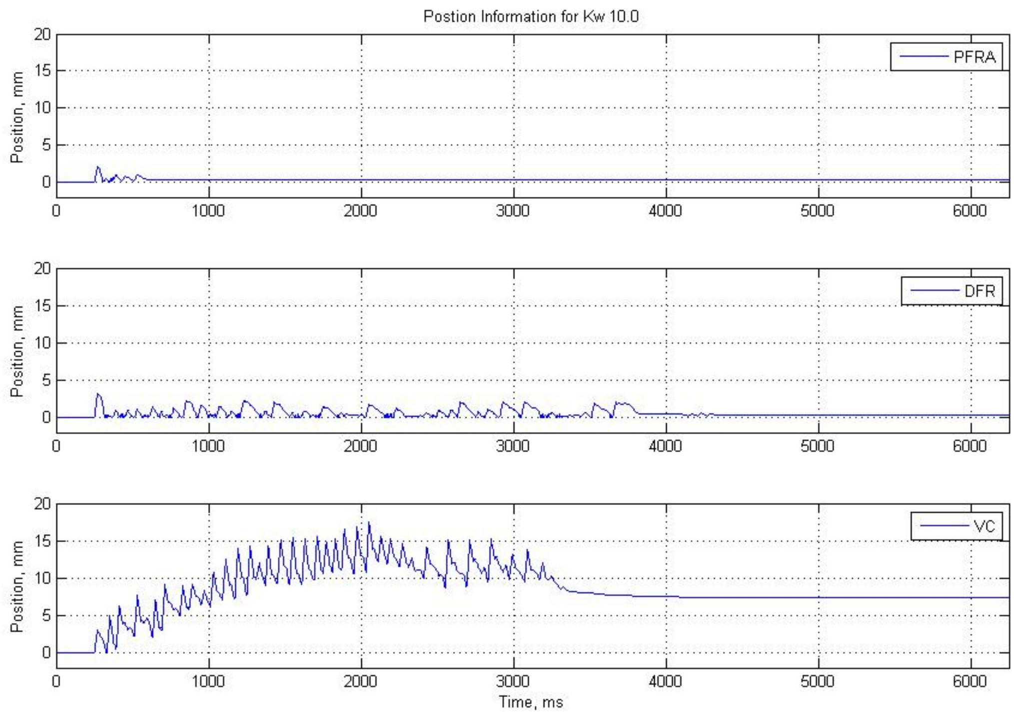

Figure 4.4: Position Information for $K_w = 10N/mm$

contact force: the direct force reflection and the projection-based component. According to Equation 2.14, higher the value of α, the greater the effect of direct force reflection component on the final force reflected to the haptic device, with the extreme case of α = 1, which reduces the PFRA to DFR. Experiments were carried out for K_w = 5 N/mm for an update rate of 50 Hz, with values of α chosen as 0.2, 0.5, 0.7 and 1.0. From the results presented in Figure 4.11, it is clearly apparent that the reflected force suffers from a decrease in stability as the value of α is increased. The reflected force is most stable for α = 0.2, while its stability is poorest for α = 1.0. Similarly, Figure 4.12 shows that the end effector of the haptic device suffers from the least oscillations for the smallest value of α chosen. This effect was evident to the user from the increased vibrations of the end effector as it was held.

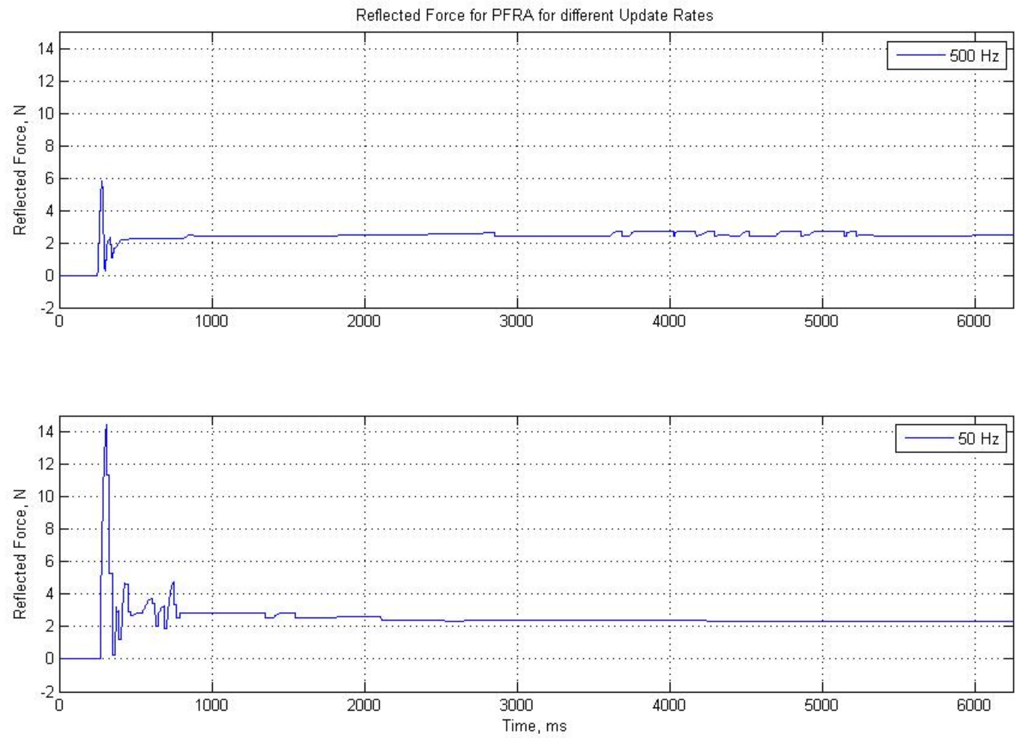

Figure 4.5: Reflected Force for PFRA for different update rates

4.5 Experiment 4: Transparency

For a haptic device to successfully represent a contact with virtual environments, transparency along with stability, is important. Transparency is the ability of a haptic system to accurately represent the properties of the virtual environment, thereby creating a realistic image to the user. The popular technique of Virtual Coupling ensures stability in haptic systems by adding an additional spring and damper, but at the same time sacrificing transparency. The DFR, as it does not use any form of modification of the reflected force, is expected to have a high level of transparency. The transparency levels of the PFRA for teleoperation systems is high, but for haptic systems it was an unknown quantity. Transparency is compared based on the apparent stiffness (Equation 3.10) of the techniques. The closer the value of apparent stiffness to the actual stiffness, the more transparent the tech-

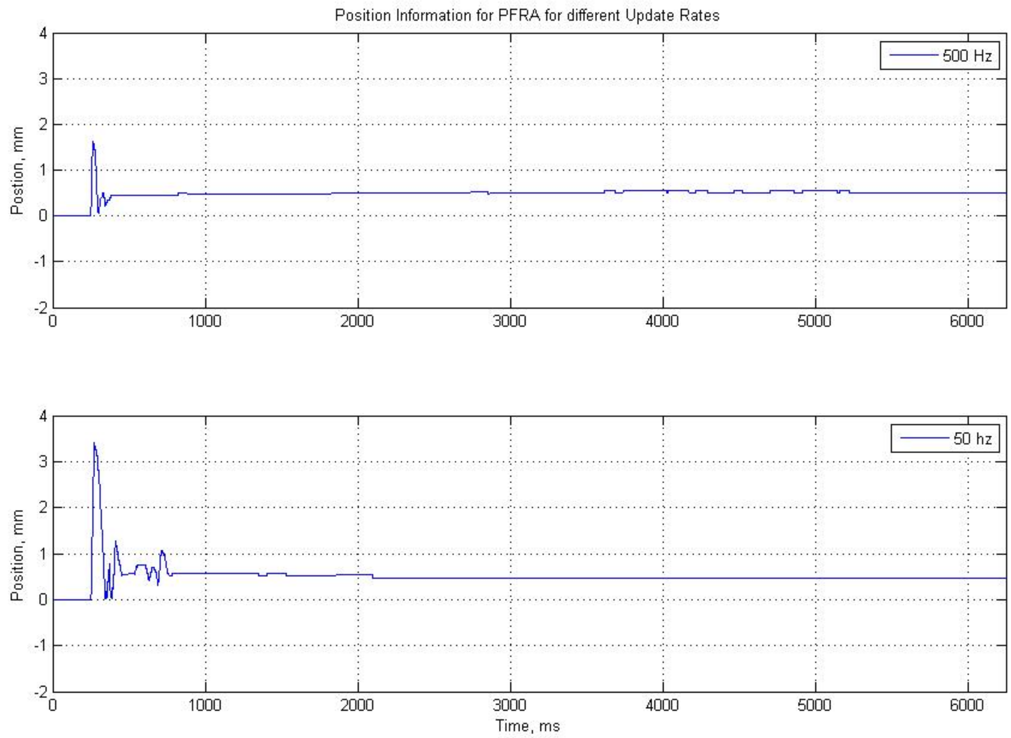

Figure 4.6: Position Information for PFRA for different update rates

nique is. The data for these apparent stiffness are presented in Table 4.1. As their apparent stiffness are equal to the actual stiffness, the transparency levels of the DFR and PFRA are said to be perfect. However, for the VC, the apparent stiffness is low compared to the actual stiffness, resulting in a low value of transparency. Not only that, the transparency levels for VC actually decreases as the stiffness of the virtual wall is increased.

4.6 Conclusion

Experiments were carried out addressing the performance of three different techniques: the virtual coupling, the projection based force reflection algorithm, and the direct force reflection, in the case where there is no time delay between the haptic device and the virtual

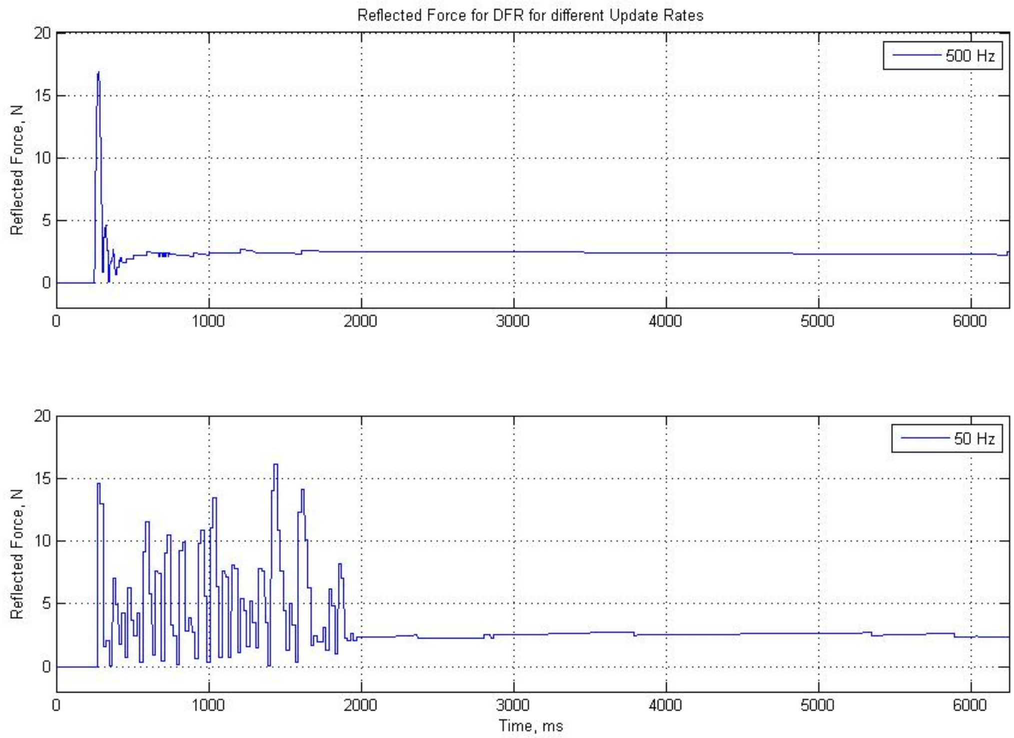

Figure 4.7: Reflected Force for DFR for different update rates

environment. Results of the experiments showed that the PFRA performs better for both low and high values of wall stiffness and update rates than the DFR and VC. It is also significantly more transparent than the VC for all values of wall stiffness under consideration during the experiments. The performance of the PFRA was shown to be dependant on the value of the weighting parameter α.

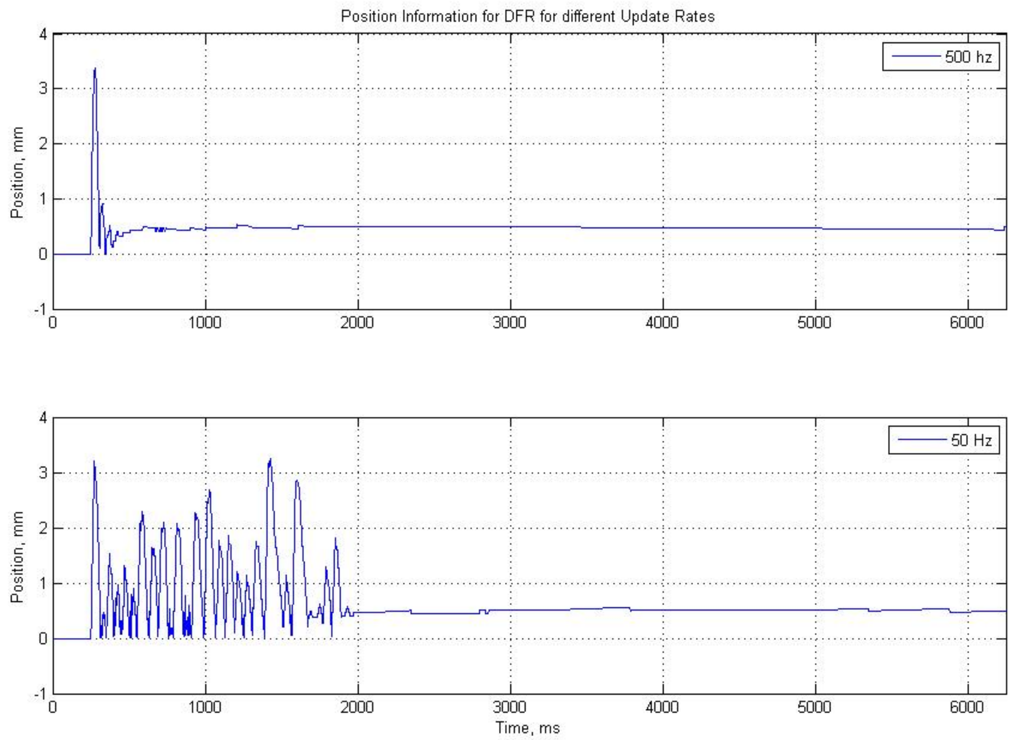

Figure 4.8: Position Information for DFR for different update rates

Table 4.1: Actual and Apparent Stiffness for Non-delayed Case

Actual stiffness (N/mm)	Apparent stiffness - PFRA (N/mm)	Apparent stiffness - DFR (N/mm)	Apparent stiffness - VC (N/mm)
3.0	3.0	3.0	0.7461
4.0	4.0	4.0	0.7993
5.0	5.0	5.0	0.833
6.0	6.0	6.0	0.8571
8.0	8.0	8.0	0.8889
10.0	10.0	10.0	0.9091

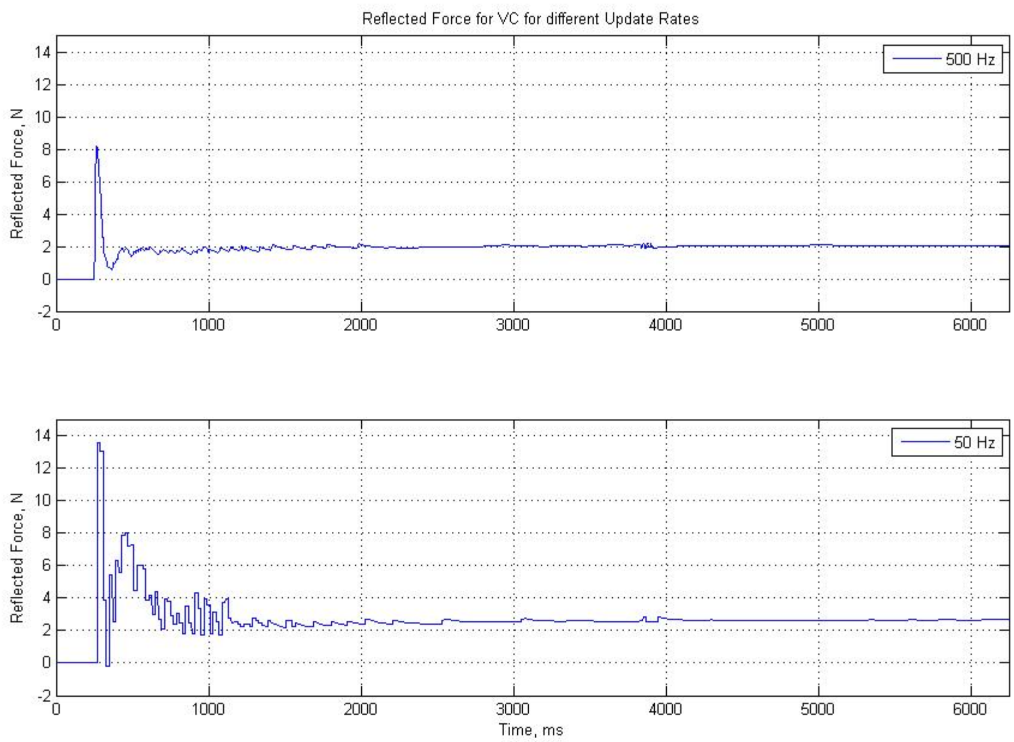

Figure 4.9: Reflected Force for VC for different update rates

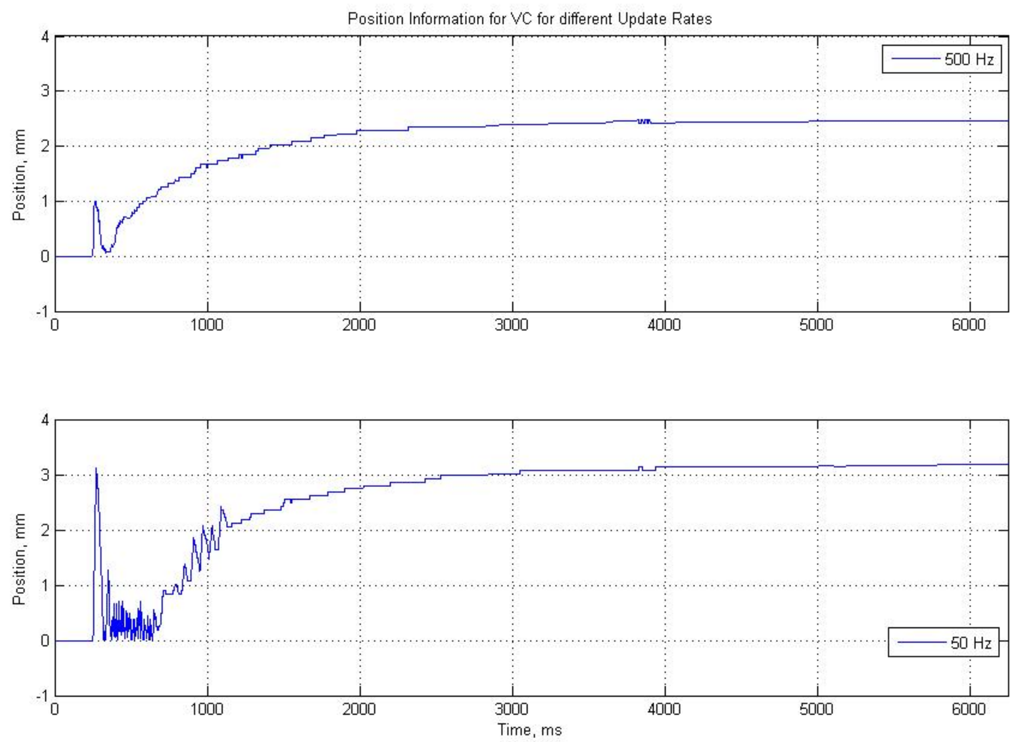

Figure 4.10: Position Information for VC for different update rates

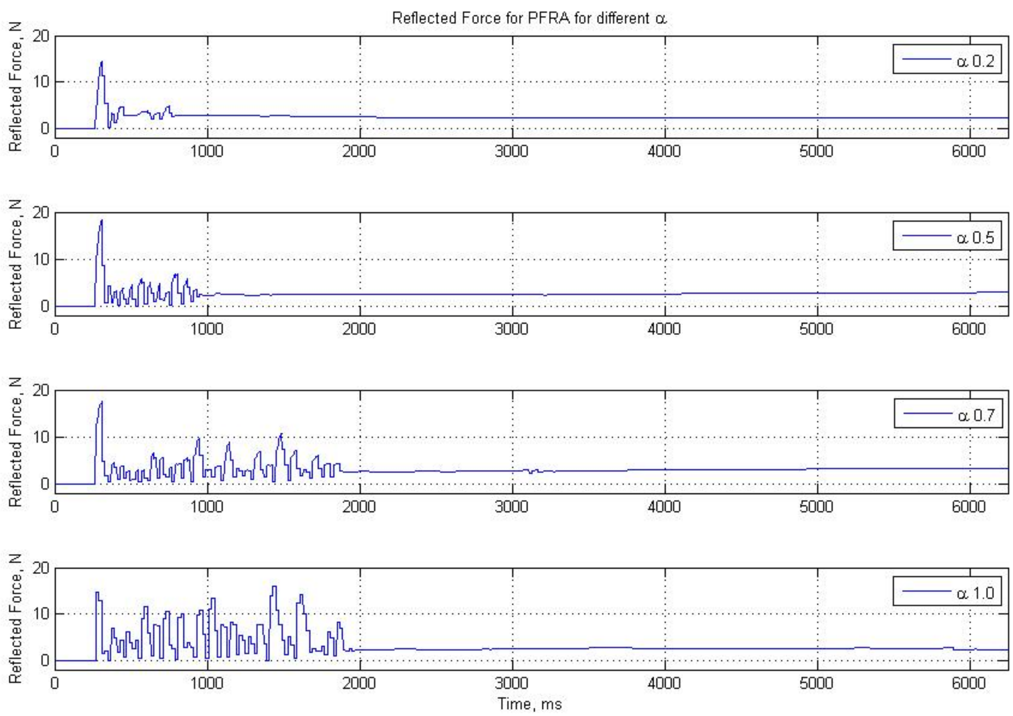

Figure 4.11: Reflected force for different values of α

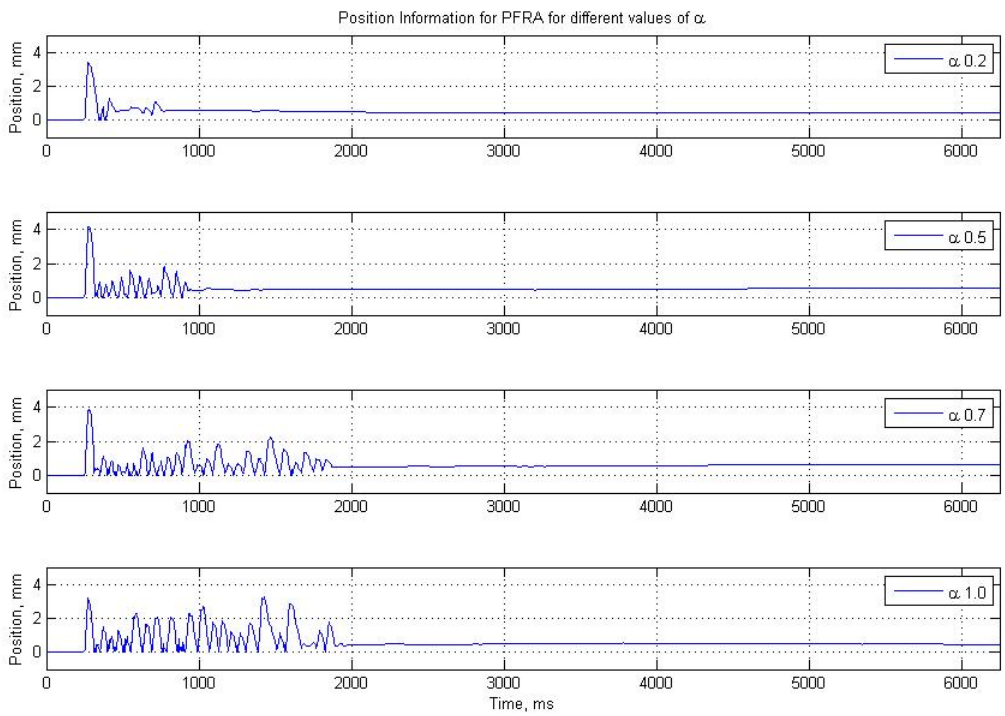

Figure 4.12: Position for different values of α

Chapter 5

Haptic Interaction with Communication Delays

5.1 Introduction

The second section of the results presents a comparative experimental study of three techniques: the Wave Variable (WV) presented in [64], the Projection based Force Reflection Algorithm (PFRA) presented in [65] and the Direct Force Reflection (DFR) technique, in improving stability and maintaining transparency in haptic interactions in the presence of significant irregular communication delay. A variety of parameters were chosen to obtain a detailed view of the performances of the techniques, including virtual wall stiffness, update rates and delay times. The performance of the PFRA was studied further under varying values of the parameter α. A comparison of the transparency was carried out based on different wall stiffness and delay variation.

5.2 Delay Pattern

Like all applications operating over the Internet, haptic interactions taking advantage of an Internet link suffers from stability and performance deterioration because of random communication delay. In particular, time varying communication delay can introduce energy into the system [66]. The purpose of the following experiments is to find the effect of different techniques to overcome the instability caused by the introduction of this extra energy. To simulate the random delay typical for communication over the Internet, a random number generator was used. The output of the random number generator varied within a predetermined range. These random numbers were then added to an integer number which represented the minimum delay. The randomness of the delay was ensured by using the current time as the seed of the generator. The generated delay is considered as the round trip delay. An example of a typical delay used in the experiments are given below. Minimum round trip delays were chosen at values of 100 ms, 200 ms and 500 ms, while the variation in delay were set at 10 ms, 50 ms and 100 ms.

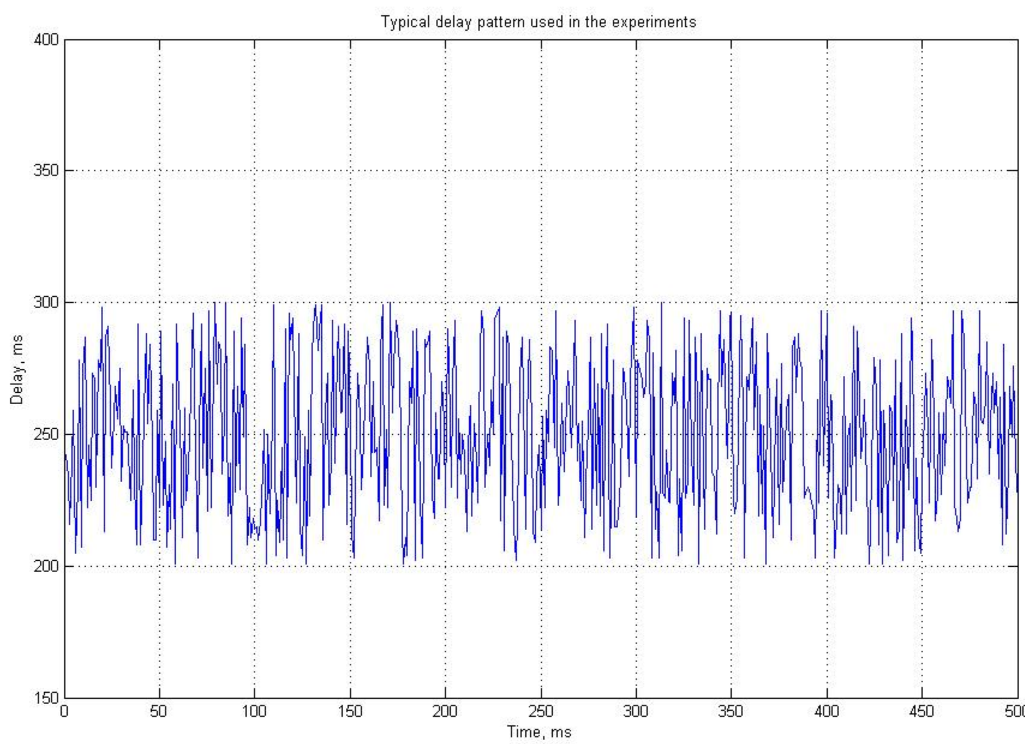

Figure 5.1: A Typical Pattern of the Delay used in the Experiments

5.3 Experiment 1: Virtual Wall Stiffness

The first set of experiments carried out was focussed on analysing the effect of a change in stiffness of the virtual wall on the performance of the different techniques. For all the experimental results presented in this section, the delay was set to a minimum of 200 ms with a variation of 50 ms. The update rate of the reflected force was chosen as 500 Hz. The experiment was carried out for two different stiffness of the virtual wall: 1 N/mm and 2 N/mm. The damping of the virtual wall was set at 0.005 Ns/mm.

Figure 5.2 presents the change in performance of the wave variable technique when the stiffness of the virtual wall is changed . The value of the wave impedance in this case was chosen as 0.01, as it was observed that higher values of the wave impedance caused oscillations during contact, while lower values of this parameter caused oscillations during free space movement. The stability of the wave variable technique decreases as the stiffness is increased, which is apparent from the increased oscillations in the curve for reflected force.

The figure for the position information of the end effector of the haptic device is presented in Figure 5.3. The position information is the amount of penetration by the end effector into the virtual wall. The loss of stability with increasing stiffness can be better visualized from this figure where the increased stiffness causes the end effector to suffer from more vibrations, which can also be felt by the user during the experiment.

In Figure 5.4, the performance of the PFRA, where the value of the parameter α was chosen as 0.2, is shown as a function of changing wall stiffness. The reflected force undergoes an increase in oscillation as the stiffness is increased, but it becomes stable faster than the WV technique, for higher values of stiffness.

The position information for the end effector for the PFRA is shown in Figure 5.5, where the decrease in stability is more clearly depicted. However, as can be seen from the figure and comparing the result with the results presented in Figure 5.3, it is clearly evident that the PFRA enables the end effector of the device to become stable faster and also has a

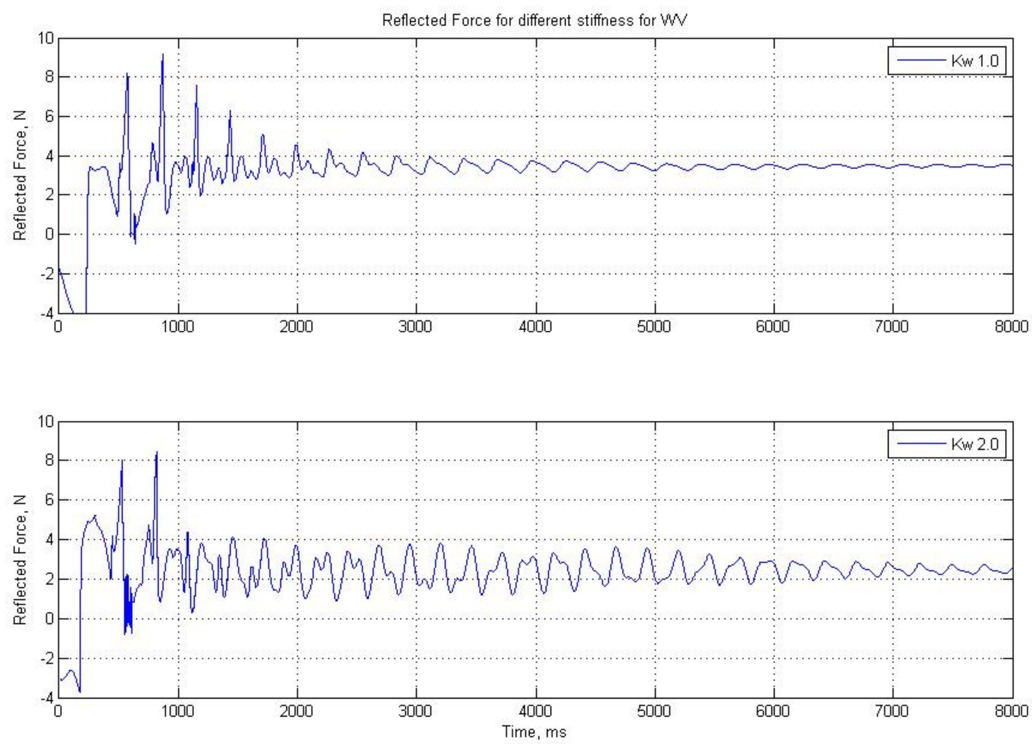

Figure 5.2: Performance of the Wave Variable technique as the stiffness of the virtual wall is increased.

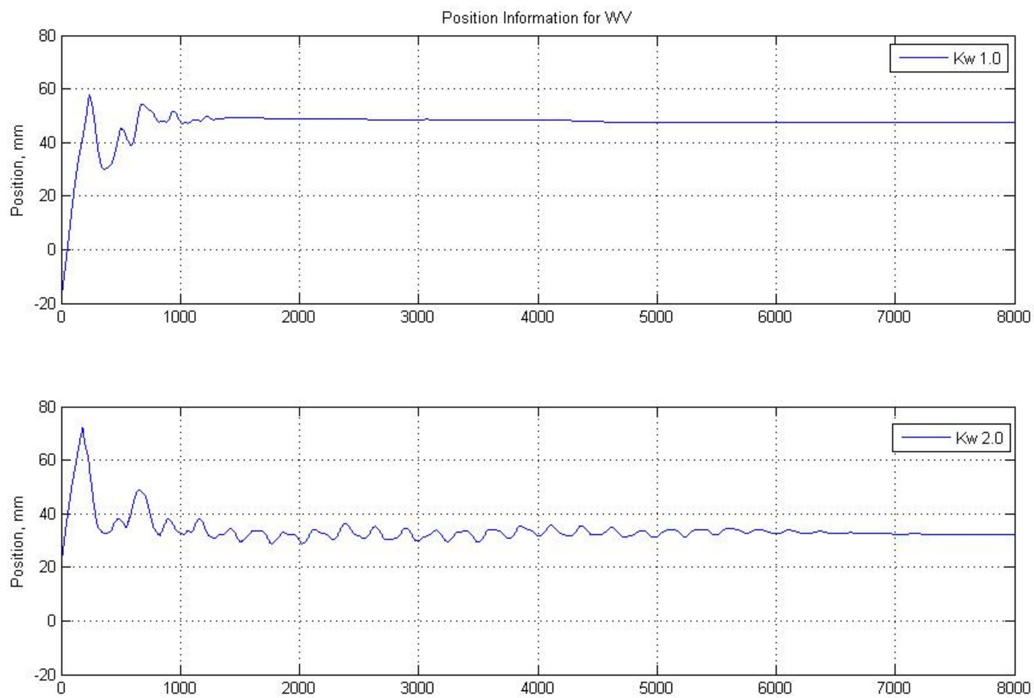

Figure 5.3: Position of the End Effector of the Haptic Device for the Wave Variable technique as the stiffness of the virtual wall is increased.

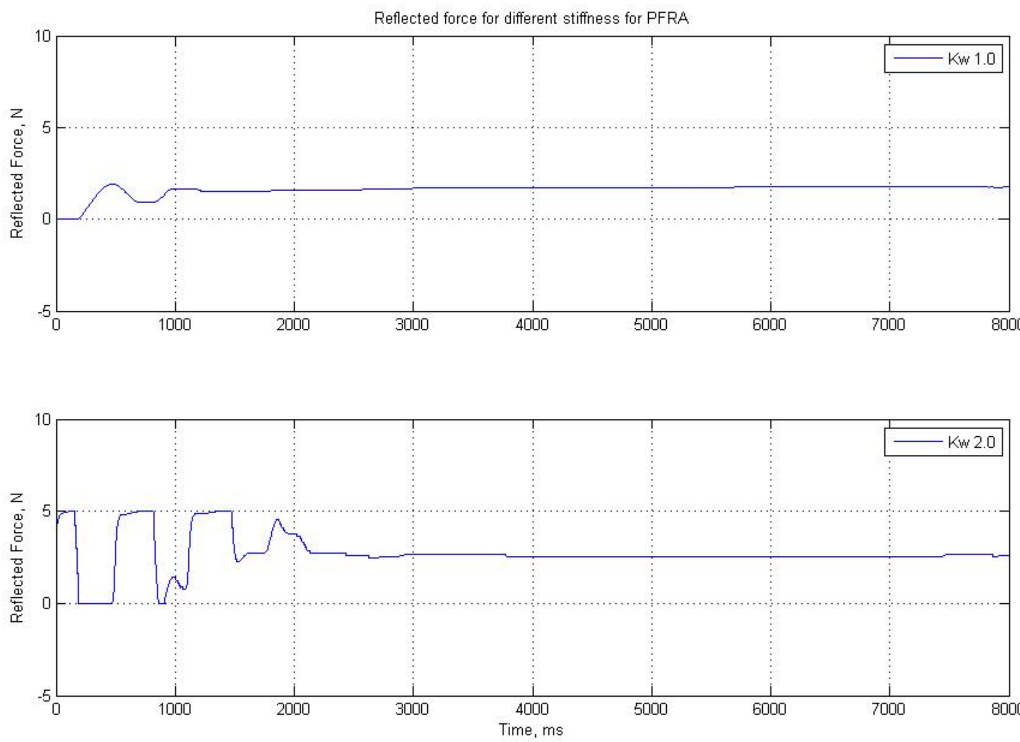

Figure 5.4: Performance of the Projection based Force Reflection technique as the stiffness of the virtual wall is increased.

smaller peak value of oscillation.

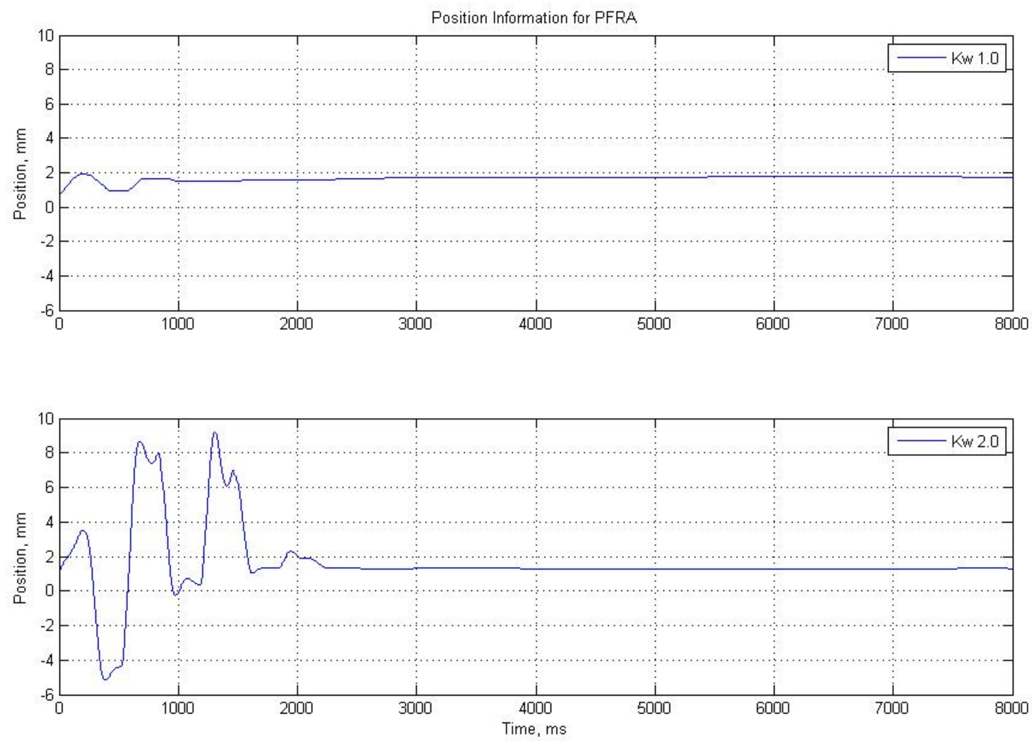

Figure 5.5: Position of the End Effector of the Haptic Device for the Projection based Force Reflection technique as the stiffness of the virtual wall is increased.

Figure 5.6 presents the results for the DFR technique when the stiffness of the virtual wall is increased. For this case, the value of α is 1.0, as this is the boundary case of PFRA. From the figure it is apparent that the haptic system suffers significant deterioration in performance in terms of stability for reflected force as the virtual wall becomes stiffer. The position information presented in the Figure 5.7 further corroborates this observation, showing that the end effector suffers from oscillations for a longer amount of time as the wall stiffness is increased. This effect was clearly experienced by the user as he held on to the device. Such oscillations resulted also in increased fatigue for the user.

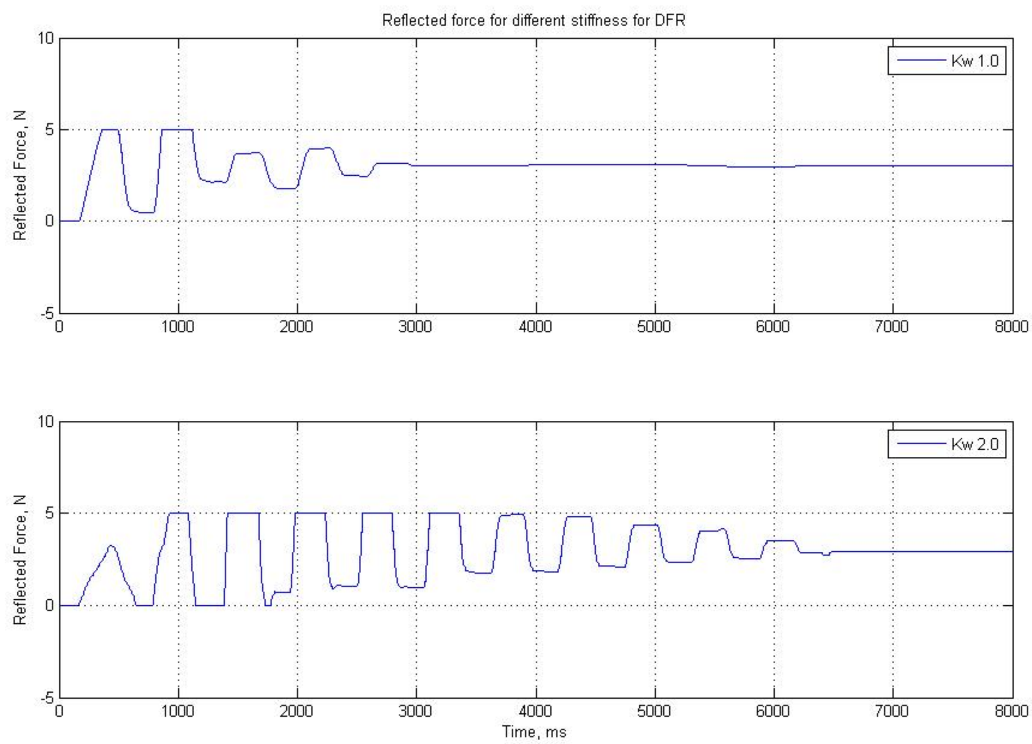

Figure 5.6: Performance of the Direct Force Reflection technique as the stiffness of the virtual wall is increased.

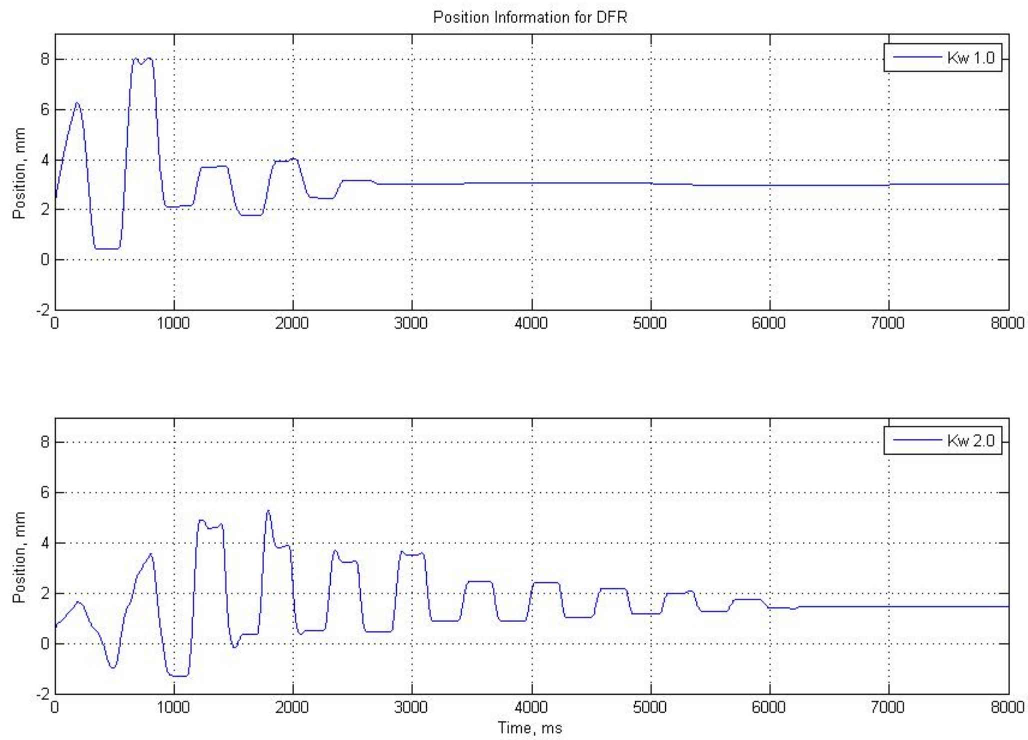

Figure 5.7: Position of the End Effector of the Haptic Device for the Direct Force Reflection technique as the stiffness of the virtual wall is increased.

5.4 Experiment 2: Update Rates

The performance of the three techniques were also analysed for different update rates. Two update rates of the reflected force were chosen for consideration: 500 Hz and 50 Hz. The performance of the techniques were compared in terms of both reflected force and penetration of the end effector into the virtual wall, which was described as the position information of the end effector. The delay in these experiments were set to a minimum of 100 ms with a variation of 50 ms. The virtual wall stiffness was set at 1 N/mm, and the damping at 0.005 Ns/mm.

The performance of the wave variable technique in terms of the reflected force is shown in Figure 5.8. For this experiment, the wave impedance was set at a value of 0.005. From the figure it is apparent the wave variable technique suffers minimal effects due to the change in update rates. This is in direct contradiction to the conclusions reached in [58], where it is stated that lower update rates are one of the reasons for the loss of stability.

The information regarding the position of the end effector of the haptic device when the update rate of the reflected force is changed is presented in Figure 5.9. These figures further support the results presented in Figure 5.8, that the change in update rates has minimal effect on the performance of a haptic device when wave variables are used to stabilize the system.

The results of the effect on the reflected force for a change in update rates for PFRA with $\alpha = 0.2$, are presented in Figure 5.10. The results of the experiment show that the reflected force suffers from decrease in stability due to the change in update rates for the reflected force. However, when the results in this figure are compared to those presented in Figure 5.8,it is clearly evident that reflected force becomes stable faster for the PFRA than the WV technique, even for lower update rates.

From the results presented in Figure 5.11, which shows the position information related to the PFRA when the update rate of the reflected force is changed, it can be seen that the end effector suffers from greater oscillations for lower update rates. However, both the

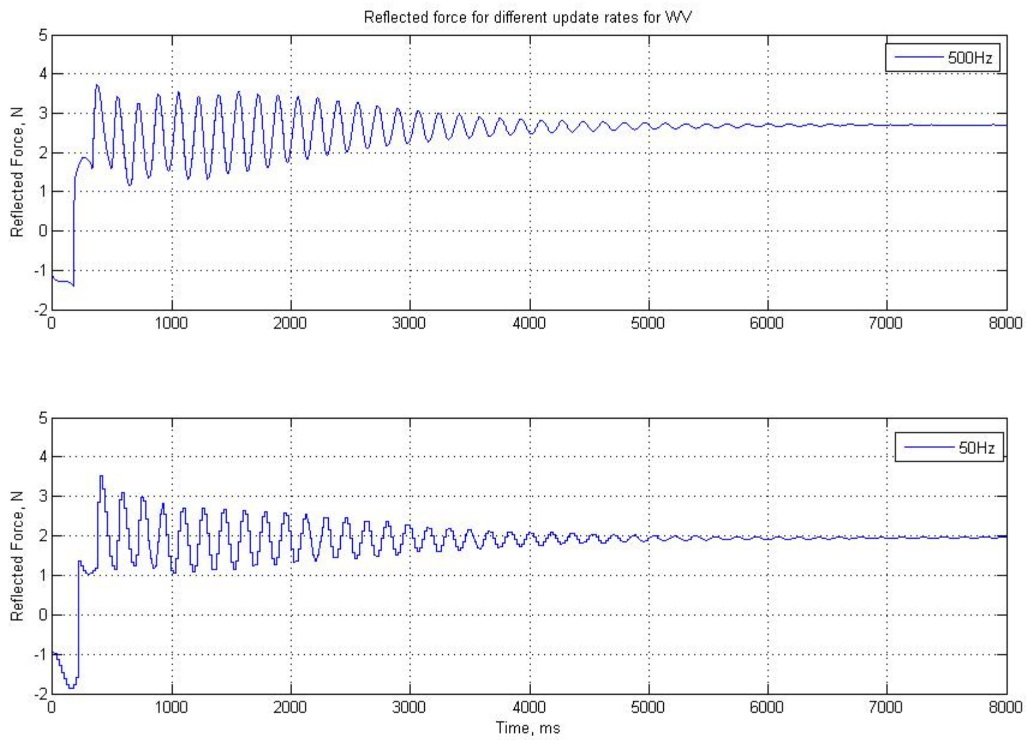

Figure 5.8: Performance of the Wave Variable technique as the Update Rate of the Reflected Force is changed.

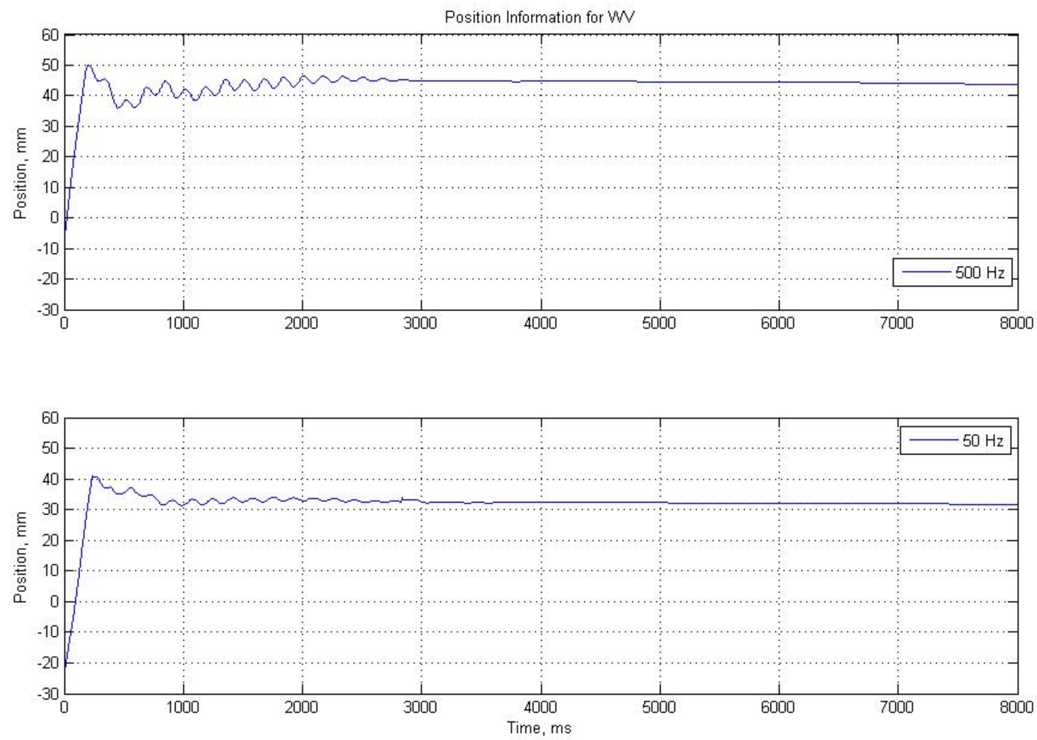

Figure 5.9: Position of the End Effector of the Haptic Device for the Wave Variable technique as the Update Rate of the Reflected Force is changed.

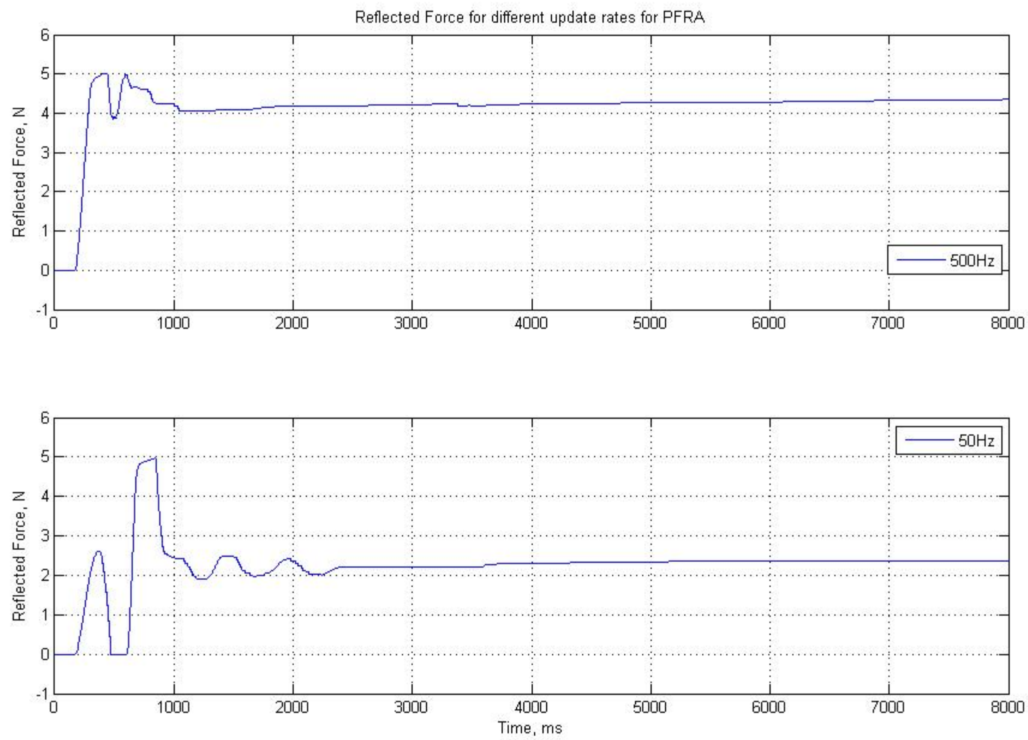

Figure 5.10: Performance of the Projection based Force Reflection technique as the Update Rate of the Reflected Force is changed.

duration of the oscillations and the amount of penetration by the end effector into the virtual wall is much less compared to the corresponding values for the WV technique.

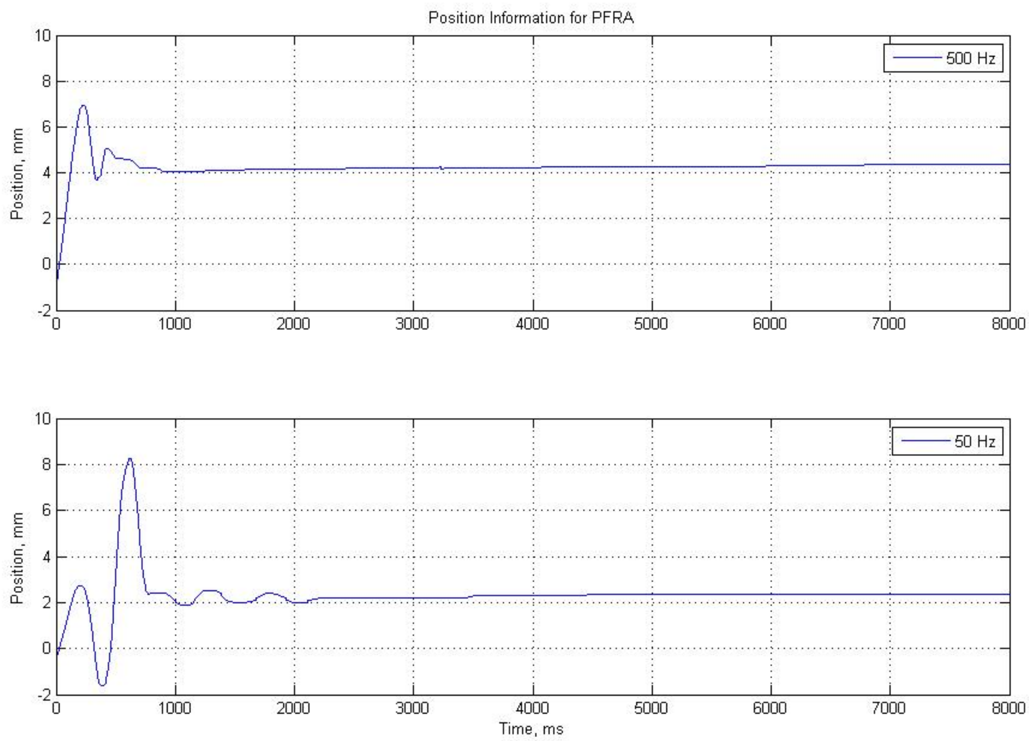

Figure 5.11: Position of the End Effector of the Haptic Device for the Projection based Force Reflection technique as the Update Rate of the Reflected Force is changed.

Finally, the results for DFR, with $\alpha = 1.0$, for different update rates are presented. Figure 5.12 presents the results for the reflected force. The results in this figure depicts clearly the significant dependence of the reflected force for DFR on the update rate of the force. A decrease of the order of 10 for the update rate causes the performance of the reflected force in terms of stability to deteriorate greatly. The position information for the DFR presented in Figure 5.13 also supports the results of Figure 5.12. From this figure it is clear that the end effector of the haptic device suffers from a greater degree of oscillations for lower update rates of the reflected force. This was also very readily experienced during the performance of the experiment.

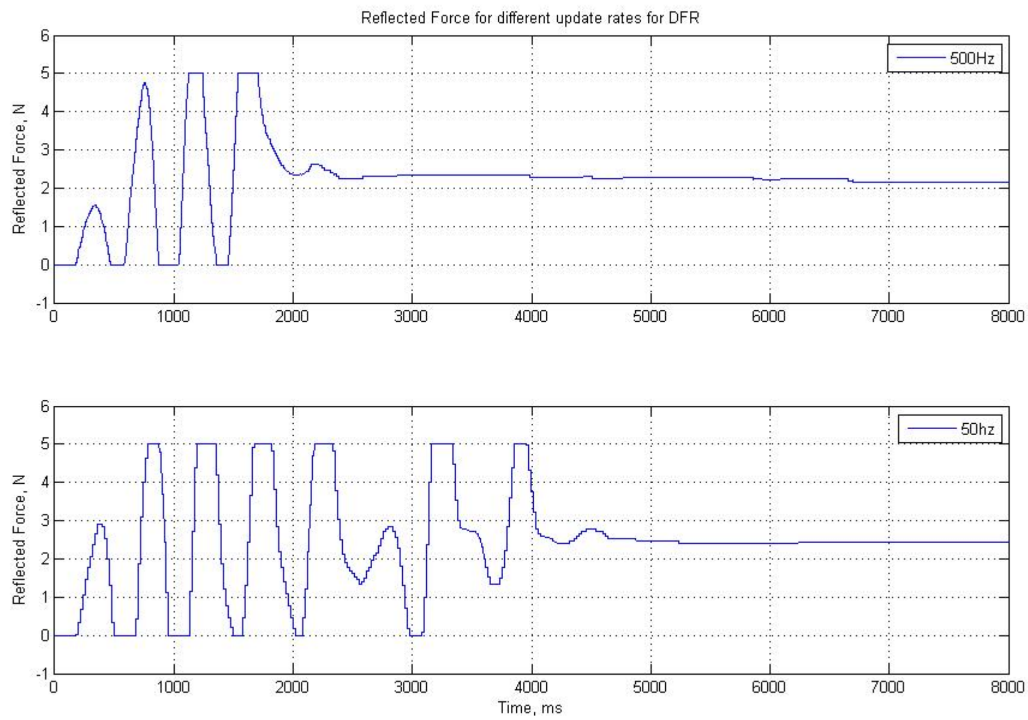

Figure 5.12: Performance of the Direct Force Reflection technique as the Update Rate of the Reflected Force is changed.

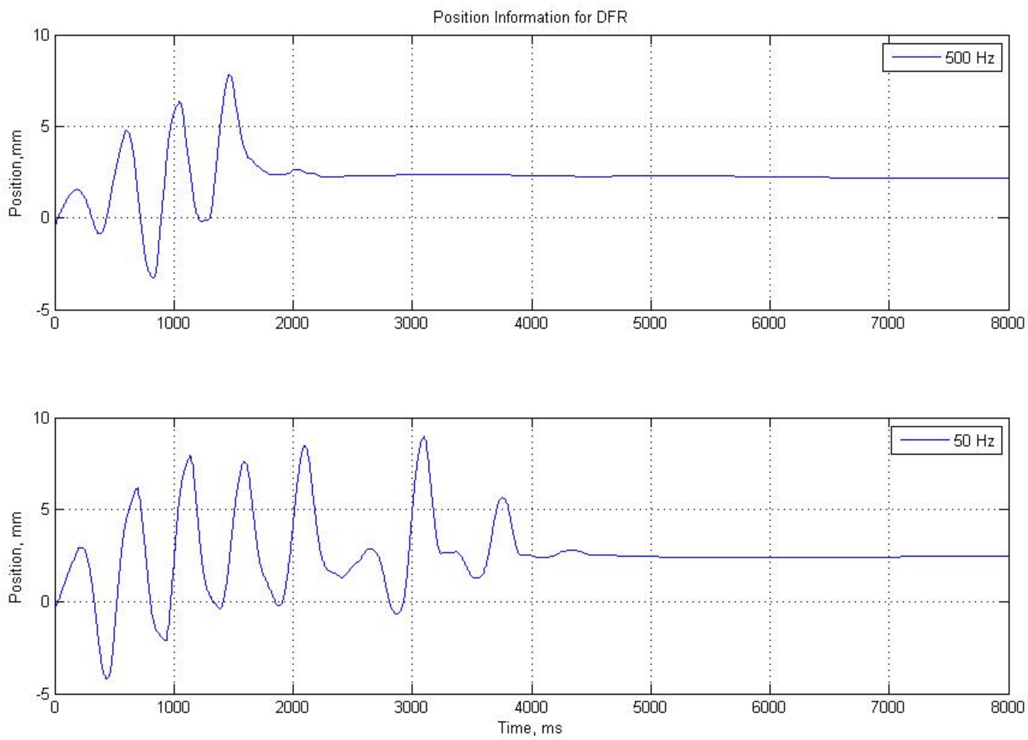

Figure 5.13: Position of the End Effector of the Haptic Device for the Direct Force Reflection technique as the Update Rate of the Reflected Force is changed.

5.5 Experiment 3: Delay

In the third set of experiments, the performance of the three techniques are compared for different delay times. The objective was to observe what the effect of different delay times will have on the reflected force and the amount of penetration by the end effector of the haptic device into the virtual wall. The minimum values of delay chosen were 100 ms and 500 ms with a variation of 500 ms for both cases. The stiffness of the wall is set at 1 N/mm and the damping is 0.005 Ns/mm. The update rate of the reflected force is set at 500 Hz. For experiments related to WV, the wave impedance was set at 0.005 and 0.0175 for minimum delays of 100 ms and 500 ms respectively.

The first figure in this set of experiments, Figure 5.14 shows the performance of the three techniques in terms of the reflected force for a minimum delay of 100 ms. This result shows that the PFRA, where α has a value of 0.2, is the fastest to reach a stable value for the reflected force. The peak value of the oscillation in the reflected force for DFR, with α = 1.0, is the greatest among the three techniques. For the WV technique, however, the peak value is the lowest. When the minimum delay is increased to 500 ms, the results show a marked change in behaviour of the techniques. These results are presented in Figure 5.15. While the performance of all three techniques suffer some degree of deterioration, it is evident from the figure that the performance of the WV techniques in terms of reflected force suffers the greatest, becoming very unstable during the period of observation. The DFR technique also suffers significantly, which is clearly visible from the fact that it requires a long time to become stable. The PFRA technique suffers the least degradation in performance, the time required for the reflected force to reach a stable value not increasing greatly.

The position information for the three techniques for the two delay times under consideration are presented in Figures 5.16 and 5.17. In Figure 5.16, from the position information for a minimum delay time of 100 ms, it can be seen that the end effector suffers from minimum instability among the three techniques. The WV and the DFR techniques both

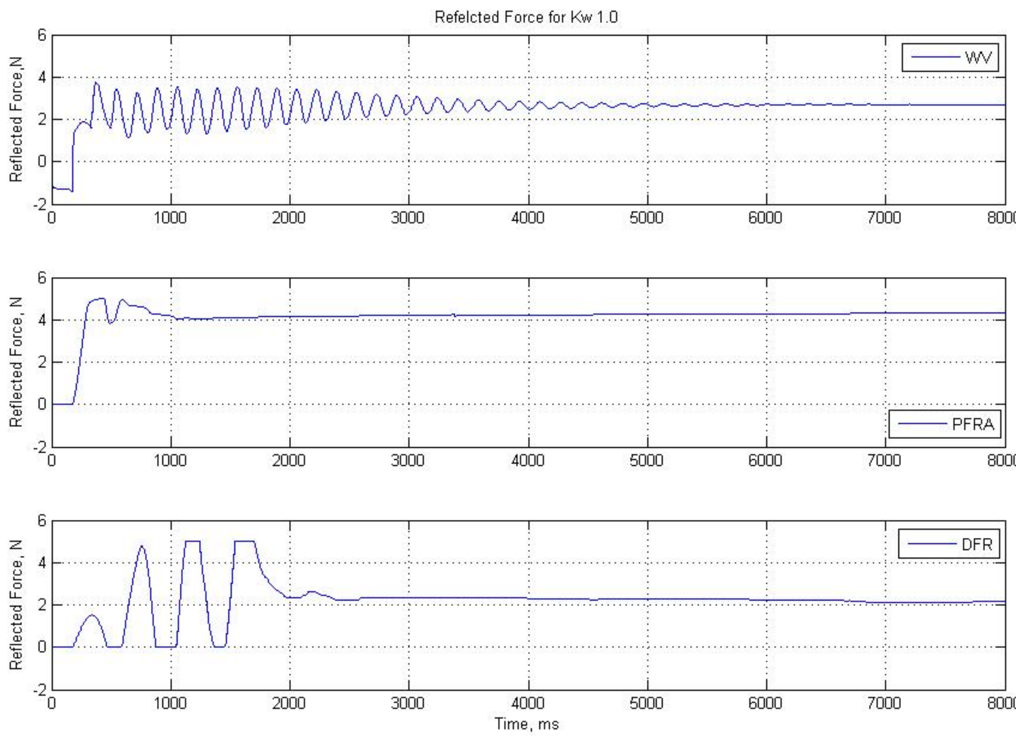

Figure 5.14: Performance of the three technique for a minimum delay of 100 ms.

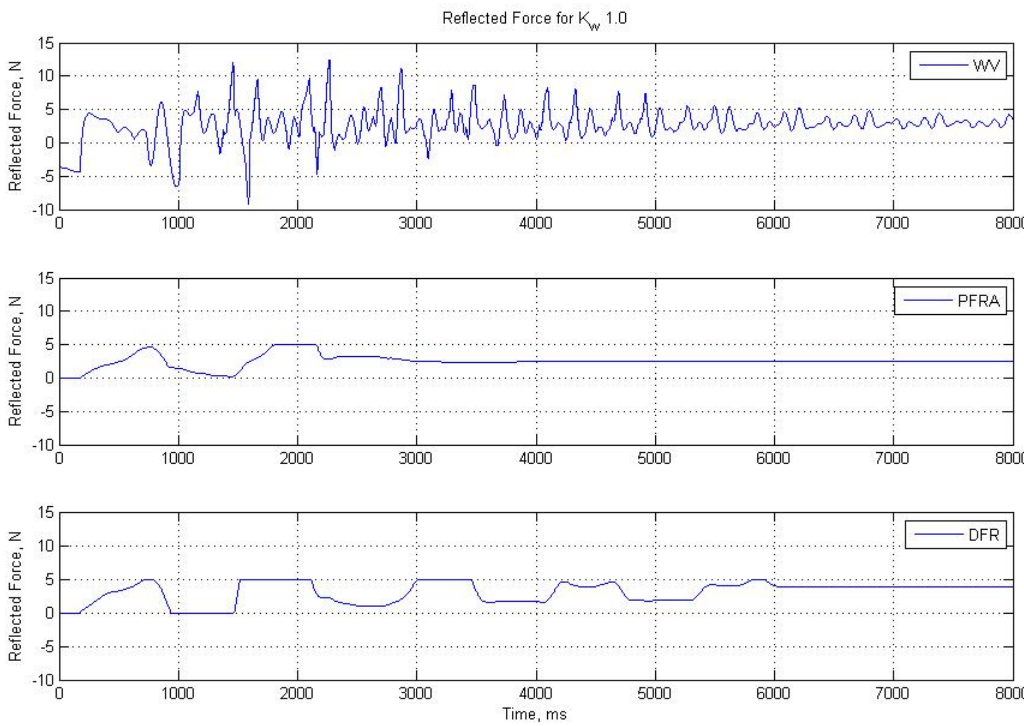

Figure 5.15: Performance of the three technique for a minimum delay of 500 ms.

suffer from greater instability than the PFRA, with the penetration of the end effector into the virtual wall is far greater than the other two techniques. When the minimum delay time is increased to 500 ms, the advantage of the PFRA is clearly evident. It is clearly visible from the figure that the PFRA enables the end effector to become stable faster. Compared to the performance of the PFRA, the DFR performs poorly, which is clear from the figure where the end effector is shown to take longer in becoming stable. At this larger minimum delay, the WV technique performs the poorest. This is clearly evident from the fact that not only does the end effector penetrates the farthest into the virtual wall, it also becomes significantly more unstable.

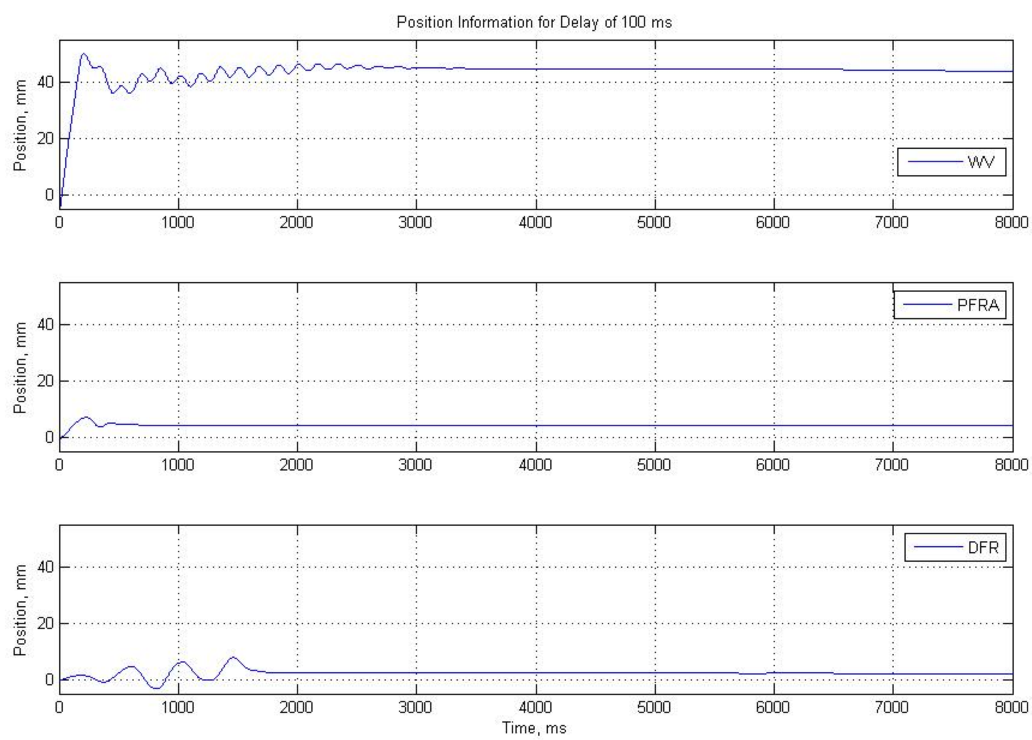

Figure 5.16: Position Information for the three technique for a minimum delay of 100 ms.

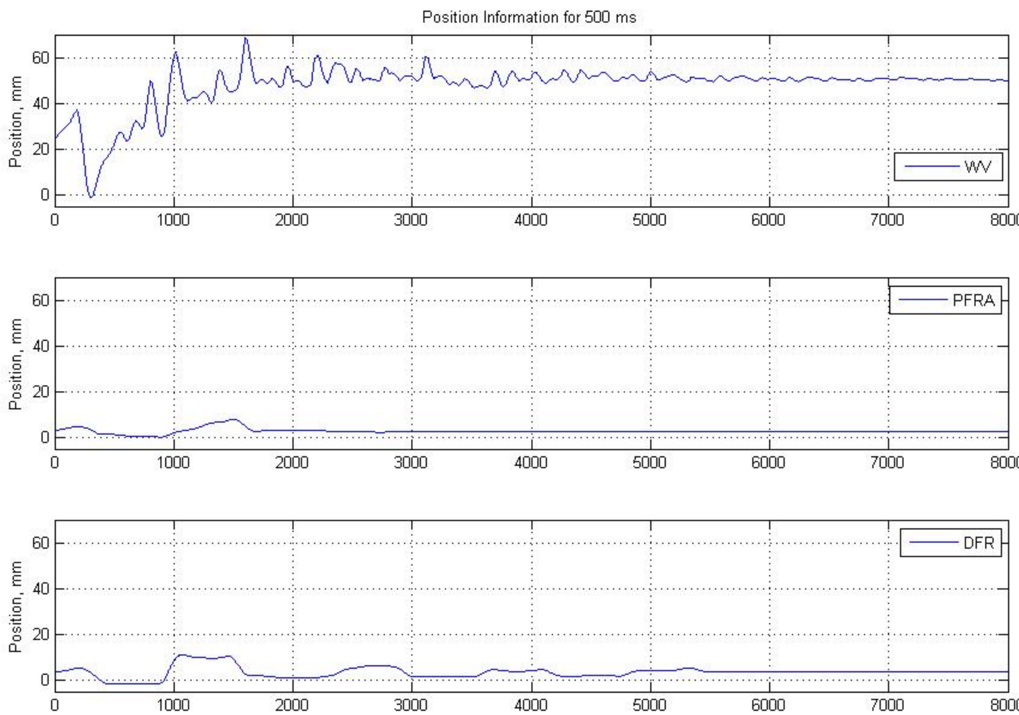

Figure 5.17: Position Information for the three technique for a minimum delay of 500 ms.

5.6 Experiment 4: PFRA Parameter α

The weighting coefficient α has a significant effect on the performance of the PFRA. This set of experiments were carried out in order to find out the extent of this effect in the presence of delay. A minimum delay of 200 ms with a variation of 50 ms is used. The virtual wall had a stiffness of 1 N/mm. The update rate of the reflected force was chosen as 500 Hz. The values of the parameter α that were chosen are 0.2, 0.5, 0.7 and 1.0. Both the reflected force and penetration into the virtual wall by the end effector were studied in order to get an informed view of the effect of change in the parameter.

Figure 5.18 presents the results for reflected force when the value of the parameter α is changed gradually. As can be seen from the sequence of plots, the performance of PFRA decreases as the α increases from a small value of 0.2 to 1.0, which corresponds to the DFR. For the smallest value under consideration, the reflected force experiences the least oscillations and becoming stable fastest.

The position information presented in Figure 5.19 depicts the same pattern of behaviour for the PFRA. For a small value of α, for instance 0.2, the PFRA is relatively stable, with the end effector coming to stable position quickly. However, as α assumes a larger value, the oscillations become larger, with the end effector requiring a longer time to settle to a stable position.

5.7 Experiment 5: Delay Variation

In order to study the performance of the different techniques used for haptic systems with time delay, different delay times with different delay variations were used. It was seen from the results that these variations had an effect on the transparency of the system. As the delay variation increases from 10 ms to 100 ms, the apparent stiffness for the WV tends to decrease. However, for PFRA and DFR, the change in delay variation has no effect. The

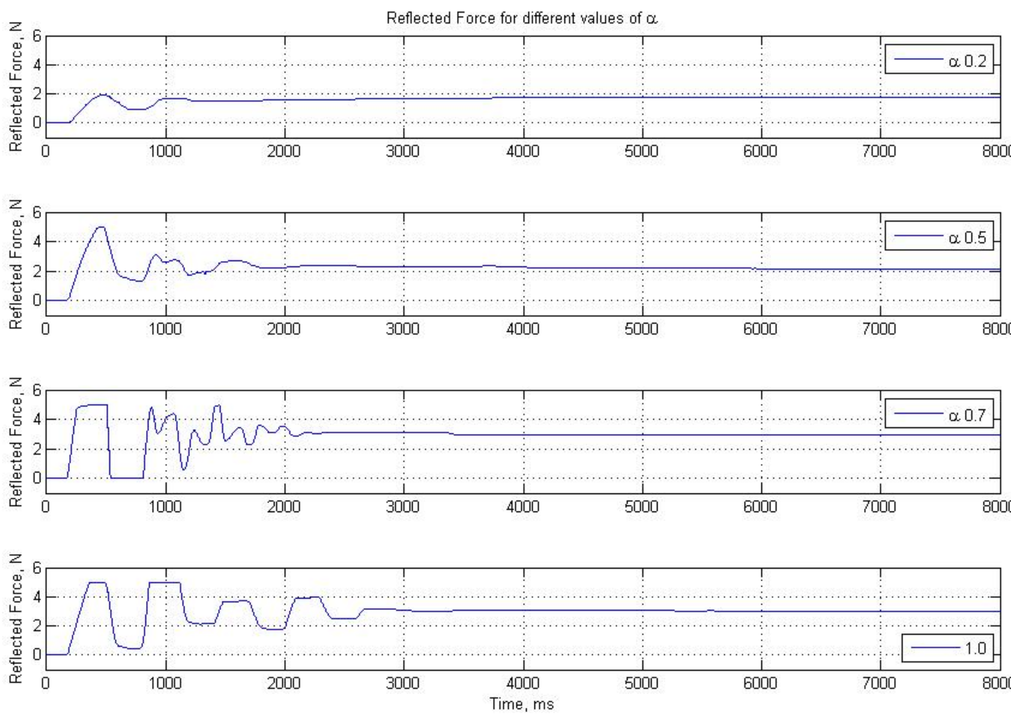

Figure 5.18: Reflected Force for the different values of α

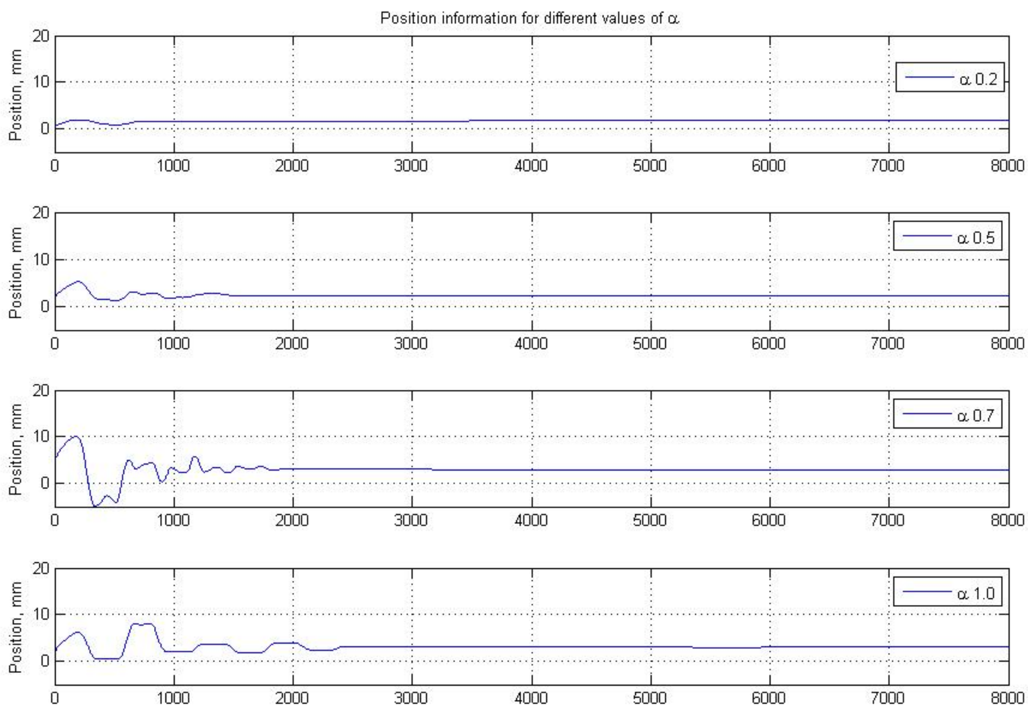

Figure 5.19: Position Information for the different values of α

Table 5.1: Apparent Stiffness for Delay Variations

Actual Stiffness 1.0			
Delay Variation	WV	PFRA	DFR
200+10	0.089	1.000	1.000
200+50	0.075	1.000	1.000
200+100	0.0643	1.000	1.000
500+10	0.0675	1.000	1.000
500+50	0.0620	1.000	1.000
500+100	0.0580	1.000	1.000

results are placed in Table 5.1.

The variation and the difference in apparent stiffness are shown in Figures 5.20 and 5.21.

5.8 Experiment 6: Apparent Stiffness

The apparent stiffness was calculated for the different actual stiffness for the the three techniques. The results presented in Table 5.2 clearly show that the WV technique suffers from severe lack of transparency. This results in a softer than realistic feeling of the haptic interaction with the virtual wall. It can be seen also from the table that the lack of transparency becomes more severe for higher values of stiffness for WV. Both the DFR and the PFRA, on the other hand, are shown to be perfectly transparent in the sense that the apparent stiffness in the steady state is equal to the actual stiffness of the virtual wall, which results in more realistic feeling of the haptic interaction.

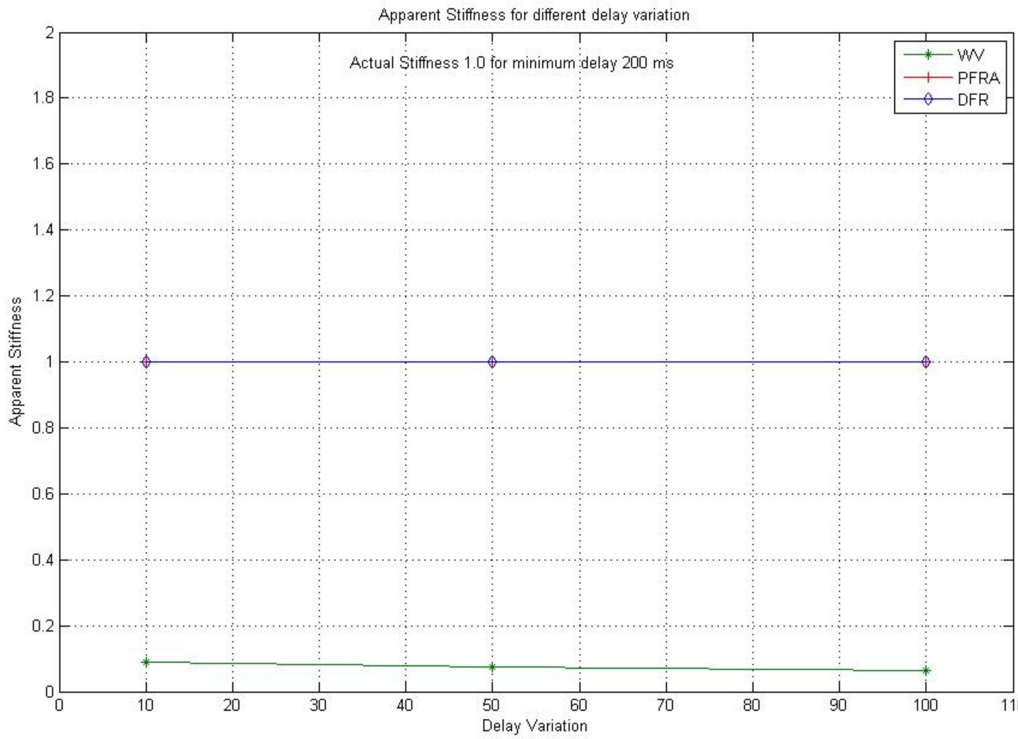

Figure 5.20: Apparent Stiffness for Delay Variations for Minimum Delay of 200 ms

Table 5.2: Actual and Apparent Stiffness

Actual Stiffness	Apparent Stiffness		
	WV	PFRA	DFR
1.0	0.0075	1.000	1.000
2.0	0.081	2.000	2.000

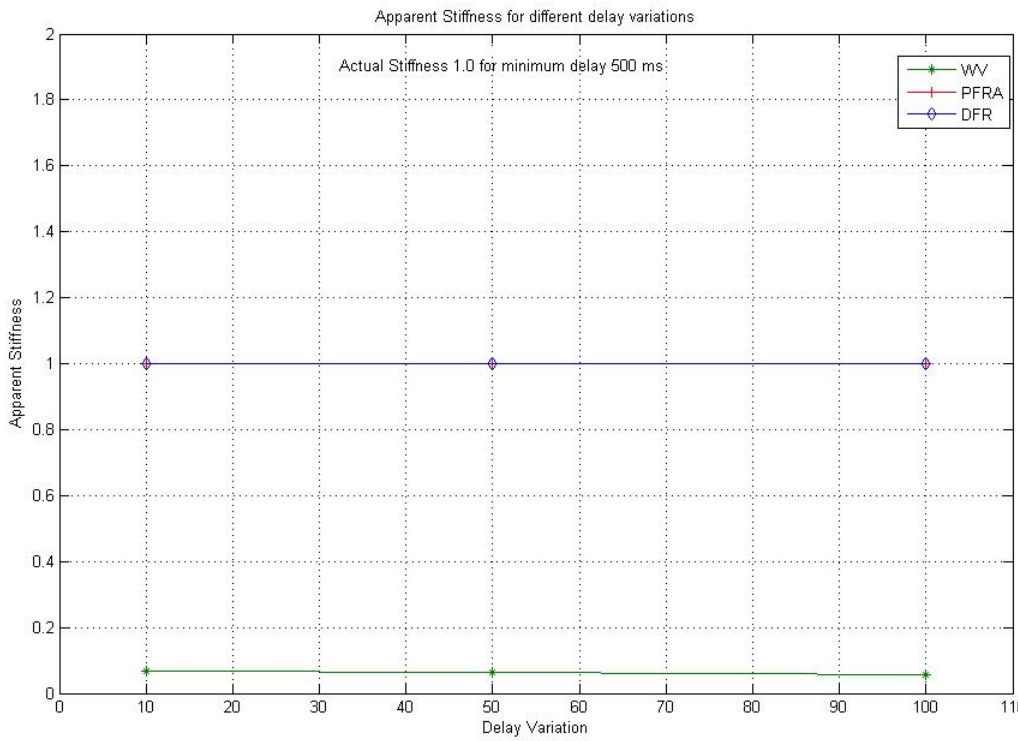

Figure 5.21: Apparent Stiffness for Delay Variations for Minimum Delay of 500 ms

5.9 Conclusion

The results presented in this section depict the performance of a haptic system under the effect of random communication delay when three different techniques: wave variables (WV), projection based force reflection algorithm (PFRA) and direct force reflection (DFR) are used to improve the stability and transparency of the system. The PFRA is able to provide a better response for different virtual wall stiffness. For lower update rates, the PFRA is not as much affected in terms of performance as the DFR. Longer delay times cause the least deterioration for the PFRA, much less compared to the DFR and WV. The transparency offered by the PFRA is perfect, and is independent of the variation in the delay, unlike the WV technique, which has a very poor level of transparency that is dependent on the variation present in the delay.

Chapter 6

Discussion

6.1 Introduction

Performance of haptic systems suffers from the effects of sampling and quantization, which may result in the loss of stability. Conventional methods that are used to overcome this problem typically maintain stability of the haptic system by adding some form of energy dissipation. However, the improvement of stability is usually achieved at the expense of decreasing transparency. If time delays are present in the communication channels, the stability and performance of haptic systems typically deteriorate further. This thesis deals with experimental investigation of a haptic system with projection based force reflection algorithm (PFRA), which is implemented with the purpose of improving the stability without sacrificing the transparency. The proposed method is experimentally compared with some existing more conventional methods, for haptic systems with and without communication delays.

6.2 Conclusions Drawn from the Work

6.2.1 Non-Delayed Haptic Interaction

The first set of experiments carried out in this thesis deals with the case of a haptic system that interacts with a virtual wall without communication delay. Three different techniques were addressed in these experiments, specifically, the virtual coupling (VC), the projection based force reflection algorithm (PFRA), and the direct force reflection (DFR). The purpose of this set of experiments was to compare relative performances of the above mentioned algorithms in terms of stability and transparency. Specifically, the stability and performance of these algorithms were compared for different update rates, as well different stiffnesses of the virtual wall. An additional experiment has been carried out in order to find how does the change of the weighting parameter α affect the performance of the PFRA.

Experimental results for different wall stiffnesses are presented in Figures 4.1, 4.2, 4.3 and 4.4. In these experiments, the performance of the algorithms was compared for two different values of virtual wall stiffness: $K = 3$ N/mm and $K = 10$ N/mm. For the lower value of the wall stiffness $K = 3$ N/mm, the performance of the force response of VC and PFRA is comparable, while the performance of DRF is the worst. However, the situation is quite different for $K = 10$ N/mm. In this case, the performance of both DFR and VC was very poor, with only PFRA providing a good response. In terms of the position response, the PFRA performs better than the other two techniques for both levels of wall stiffness. It is specially notable that the end effector takes a longer time to reach a stable position for VC.

In order to study the effect of low update rate on the performance of haptic system, experiments were performed with two different update rates: 500 Hz and 50 Hz. The DFR behaves as expected, with its performance degrading substantially for lower update rates, as shown in Figures 4.7 and 4.8. For the VC, the performance also suffers if the update rate decreases, which can be seen in Figures 4.9 and 4.10. However, the performance deterioration for VC is less significant in comparison with the DFR. The lower update rate has the least effect on the performance of PFRA, which suffers minimal deterioration. The results for this case are shown in Figures 4.5 and 4.6. Even though the VC and PFRA performs similarly for higher update rates, the end effector takes a longer time to reach its final position for VC, as shown in Figure 4.10.

The purpose of the next experiments was to compare the transparency of the DFR, VC, and PFRA, in the steady state. The apparent stiffness, which was the ratio of the reflected force to the penetration of the device into the virtual wall, was used as a measure of transparency in these experiments. The results of this comparison is presented in Table 4.1. From these results, it is evident that the VC has very poor transparency, as the apparent stiffness is typically significantly lower than the actual one. In fact, the transparency of VC becomes poorer as the stiffness of the wall increases. Both the PFRA and the DFR, however, demonstrate perfect transparency in the sense that the apparent stiffness for these two algorithms is always equal to the actual stiffness of the virtual wall.

The last experiment in this set has been performed in order to determine the effect of the weighting parameter $\alpha \in [0, 1]$ on the performance of the PFRA. The results of this experiment are presented in Figures 4.11 and 4.12. These results show that the performance of the PFRA clearly deteriorates as $\alpha \in [0, 1]$ grows; in particular, algorithm with $\alpha = 1.0$ has clearly the worst performance.

Results from the above described experiments carried out for a haptic system with no communication delay allows the following conclusions to be drawn,

a) The PFRA is able to provide a stable response for different values of wall stiffness, suffering little loss of performance for high stiffness values. On the contrary, performance of the DFR and the VC decreases substantially as the stiffness of the virtual wall increases.

b) Decreasing the update rate has little effect on PFRA, while the performance of the VC deteriorates more significantly as the update rate decreases. The DFR suffers major performance deterioration as the update rate decreases.

c) Both the PFRA and the DFR are perfectly transparent in the steady state, while the transparency of the VC is typically very poor.

d) Proper choice of the weighting coefficient $\alpha \in [0, 1]$ is important for PFRA, as it has significant effect on its performance.

Overall, our experiments demonstrate that the PFRA is able to maintain both stability and transparency for a haptic system without communication delay for a wide range of the stiffnesses of the virtual wall, and is relatively insensitive to changes in update rate. Also, the above described experiments demonstrate that, in most cases, the PFRA clearly outperforms both the VC and the DFR in terms of stability and transparency.

6.2.2 Delayed Haptic Interaction

The presence of irregular delays in the communication channel may result in instability of a haptic system, as the delays may generate energy thus making the overall system non-passive. The second set of experiments addressed the problem of stability and transparency of a haptic system in the presence of irregular communication delays. The following three techniques were chosen for study: the wave variable scheme (WV), the projection based force reflection algorithm (PFRA), and the direct force reflection (DFR). These techniques were experimentally compared for different wall stiffness, update rates, and characteristics of communication delay. The performance of the PFRA was also evaluated for different values of the weighting parameter $\alpha \in [0, 1]$.

The performance of the three techniques were studied for two different wall stiffness of $K = 1$ N/mm and $K = 2$ N/mm, respectively. The results of these experiments are presented in Figures 5.2, 5.3, 5.4, 5.5, 5.6 and 5.7. From these results, it is evident that the response of WV suffers from deterioration of performance, especially for higher stiffness. The DFR also demonstrates similar decrease in the performance for higher values of stiffness. However, PFRA does not suffer as much as the other two, and it stabilizes fastest in terms of both force and position responses.

The effect of update rates are presented in Figures 5.8, 5.9, 5.10, 5.11, 5.12 and 5.13 for two different update rates: 500 Hz and 50 Hz. These figures show that the performance degradation is smallest for WV, followed by the PFRA. The performance of DFR suffers the most. However, in comparison with the other two techniques, the response of PFRA stabilizes faster for both the update rates.

The effect of communication delay on the performance of different techniques was also studied, with the results being presented in Figures 5.14, 5.15, 5.16 and 5.17. These figures show that the PFRA performs the best among the three techniques for both small and large values of communication delay. It stabilizes faster than WV and DFR, and with less oscillations. In fact, the performance of WV suffers significantly for large values of communication delay.

The effect of the weighting parameter α has a significant effect on the performance of the PFRA, as shown in Figures 5.18 and 5.19. The results presented in these figures show that low values of α is a necessary condition for proper operation of PFRA.

Transparency has been studied for different amounts of delay variations. From the results in Table 5.1, it can be seen that the WV suffers significantly for more irregular communication delays. This variation or randomness in delay does not have any effect on the transparency of the system when PFRA and DFR are used. This is also the case when the transparency is studied for different levels of wall stiffness, as presented in Table 5.2. From this Table, it can be seen that the performance of the system in terms of transparency does not suffer for PFRA and DFR as stiffness is increased, unlike the WV.

Results of the experiments carried out for a haptic system with irregular communication delays allow the following conclusions to be drawn:

a) The PFRA demonstrates stable response for different values of wall stiffness, without suffering from significant deterioration in performance, compared to the DFR and WV.

b) Lower update rates do not affect the performance of the PFRA and WV as much as they do for the DFR. However, the PFRA is the fastest to stabilize.

c) Large communication delays do not affect the performance of PFRA as much as they affect the performance of DFR and WV.

d) Both the PFRA and DFR are perfectly transparent regardless of the variation of communication delays. The WV algorithm demonstrates poor transparency, which further deteriorates for large variations of the communication delays.

e) Proper choice of the weighting coefficient is important for PFRA, as it has a significant effect on its performance.

These conclusions lead to the belief that the PFRA is able to better maintain both stability and transparency for a haptic system with irregular communication delays, when compared to the other two techniques under study.

6.3 Future Work

While the current thesis has focused on examining the performance of the PFRA in terms of stability and transparency of the haptic systems, it may be expanded along the following lines in future:

a) A simple virtual wall was used for experiments as it is treated as a benchmark for such studies. More complex virtual environments may be substituted for the wall in future experiments.

b) In this research, the interaction between the haptic device and the virtual wall is 1-DOF, where the contact force is generated in x-direction only. More complex interaction algorithms would be of interest to further study the performance of PFRA.

c) Instead of the pen-based master that has been used in these experiments, a different haptic display, such as the haptic glove may also be used in future studies.

Bibliography

[1] G. Niemeyer, “Using Wave Variables in Time Delayed Force Reflecting Teleoperation,” Ph.D. dissertation, Massachusetts Institute of Technology, September 1996.

[2] http://www.sensable.com/documents/images/LargePHANTOMOmniImage.jpg.

[3] M. W. Spong, S. Hutchison, and M. Vidyasagar, *Robot Modelling and Control*. John Wiley and Sons, Inc., 2006.

[4] M. C. Lin and M. Otaduy, Eds., *Haptic Rendering: Foundations, Algorithms and Applications*. A. K. Peters Ltd., 2008.

[5] “What is Haptics?” http://www.immersion.com/haptics-technology/what-is-haptics/index.html.

[6] T. A. Kern, Ed., *Engineering Haptic Devices: A Beginner’s Guide for Engineers*. Springer-Verlag Berlin Heidelburg, 2009.

[7] K. Salisbury, F. Conti, and F. Barbagli, “Haptic Rendering: Introducory Concepts,” *IEEE Computer Graphics and Applications*, vol. 24, no. 2, pp. 24–32, March-April 2004.

[8] http://www.robotics.tu-berlin.de/menue/research/wearable_haptics_for_virtual_reality/.

[9] http://cgv.kaist.ac.kr/haptic_vr.

[10] http://www.cs.unc.edu/Research/assist/et/2005/AMaze.html.

[11] http://www.sensable.com/haptic-phantom-desktop.htm.

[12] J. E. Colgate, M. C. Stanley, and J. M. Brown, “Issues in the Haptic Display of Tool Use,” in *Proceedings of the 1995 IEEE/RSJ International Conference on Intelligent Robots and Systems*, vol. 3, Pittsburgh, PA, USA, August 1995, pp. 140–145.

[13] R. J. Adams and B. Hannaford, “A Two-port Framework for the Design of Unconditionally Stable Haptic Interfaces,” in *Proceedings of the 1998 IEEE/RSJ International Conference on Intelligent Robots and Systems*, Victoria, BC, Canada, October 1998, pp. 1254–1259.

[14] ——, “Stable Haptic Interaction with Virtual Environments,” *IEEE Transactions on Robotics and Automation*, vol. 15, no. 3, pp. 465–474, June 1999.

[15] R. J. Adams, D. Klowden, and B. Hannaford, “Stable Haptic Interaction Using the Excalibur Force Display,” in *Proceedings of the 2000 IEEE International Conference on Robotics and Automation*, San Francisco, CA, USA, April 2000, pp. 770–775.

[16] R. J. Adams and B. Hannaford, “Control Law Design for Haptic Interfaces to Virtual Reality,” *IEEE Transactions on Control Systems Technology*, vol. 10, no. 1, pp. 3–13, January 2002.

[17] B. E. Miller, J. E. Colgate, and R. A. Freeman, “Guaranteed Stability of Haptic Systems with Nonlinear Virtual Environments,” *IEEE Transactions on Robotics and Automation*, vol. 16, no. 6, pp. 712–719, December 2000.

[18] S. Lertpolpairoj, T. Maneewarn, and S. Laowattana, “Realistic and Stability Performances of Haptic System with Adaptive Virtual Coupling,” in *IEEE International Conference on Industrial Technology*, vol. 1, Bangkok, Thailand, December 2002, pp. 354–358.

[19] M. H. Lee and D. Y. Lee, "Stability of Haptic Interface using Nonlinear Virtual Coupling," in *IEEE International Conference on Systems, Man and Cyberbetics*, vol. 4, October 2003, pp. 3420–3424.

[20] D. Bi, J. Zhang, and G. Wang, "Fuzzy Virtual Coupling Design for High Performance Haptic Display," in *Fuzzy Systems and Knowledge Discovery*, ser. Lecture Notes in Computer Science. Springer Berlin / Heidelberg, 2005, vol. 3613, pp. 942–949.

[21] K. Akahane, S. Hasegawa, Y. Koike, and M. Sato, "A Proposal of a High Definition Haptic Rendering for Stability and Fidelity," in *Proceedings of the 16th International Conference on Artificial Reality and Telexistence - Workshops (ICAT'06)*, Hangzhou, China, November-December 2006, pp. 162–167.

[22] G. Sankaranarayanan and B. Hannaford, "Virtual Coupling Schemes for Position Coherency in Networked Haptic Environments," in *The First IEEE/RAS-EMBS International Conference on Biomedical Robots and Biomechatronics*, February 2006, pp. 853–858.

[23] ——, "Experimental Internet Haptic Collaboration using Virtual Coupling Schemes," in *Symposium on Haptic Interfaces for Virtual Environment and Teleoperator Systems 2008*, Reno, NV, USA, March 2008, pp. 259–266.

[24] ——, "Comparison of Performance of Virtual Coupling Schemes for Haptic Collaboration using Real and Emulated Internet Connections," in *Proceedings of Robocom 2007*, Athens, Greece, October 2007.

[25] G. Bianchini, M. Orlandesi, and D. Prattichizzo", "Analysis and Design of Multicontact Haptic Systems: an LMI Approach," in *Proceedings of the 40th IEEE Conference on Decision and Control*, New Orleans, LA, USA, December 2007, pp. 5761–5766.

[26] G. Bianchini, M. Orlandesi, and D. Prattichizzo, "Stability Analysis and Design of Multi-dimensional Haptic Systems," in *Symposium on Haptic Interfaces for Virtual*

Environments and Teleoperator Systems, Reno, Nevada, USA, March 2008, pp. 177–184.

[27] ——, "An LMI Framework for Analysis and Design of Multi-dimensional Haptic Systems," in *Proceedings of the 47th IEEE Conference on Decision and Control*, Cancun, Mexico, December 2008, pp. 4564–4569.

[28] D. Šurdilović and J. Radojićić, "Robust Control of Interaction with Haptic Interfaces," in *2007 IEEE International Conference on Robotics and Automation*, Roma, Italy, April 2007, pp. 3237–3244.

[29] Y. Zhu, J. Fan, Q. Meng, J. Zhao, and H. Cai, "Transparency Oriented Virtual Coupling Design: New Approach and Application to a Novel Admittance Haptic Device," in *Intelligent Robotics and Applications*, ser. Lecture Notes in Computer Science. Springer Berlin / Heidelberg, 2008, vol. 5315, pp. 81–90.

[30] B. D. Adelstein and M. J. Rosen, "Design and Implementation of a Force Reflecting Manipulandum for Manual Control Research," in *Proceedings of DSC-Vol.42, Advances in Robotics, ASME Winter Annual Meeting*, Anaheim, CA, USA, 1992, pp. 1–12.

[31] K. Akahane, S. Hasegawa, Y. Koike, and M. Sato, "A Development of High Definition Haptic Controller," in *Proceedings of the First Joint Eurohaptics Conference and Symposium on Haptic Interfaces for Virtual Environment and Teleoperator Systems*, Pisa, Italy, March 2005, pp. 576–577.

[32] J. An and D. S. Kwon, "Stability and Performance of Haptic Interfaces with Active/Passive Actuators - Theory and Experiments," *International Journal of Robotic Research*, vol. 25, no. 11, pp. 1121–1136, November 2006.

[33] T. B. Kwon and J. B. Song, "Force Display using a Hybrid Haptic Device Composed of Motors andBrakes," *Mechatronics*, vol. 16, no. 5, pp. 249–257, 2006.

[34] C. Bullion and H. Gurocak, "Haptic Glove with MR Brakes for Distributed Finger Force Feedback," *Presence*, vol. 18, no. 6, pp. 421–433, December 2009.

[35] J. E. Colgate and J. M. Brown, "Factors Affecting the Z-Width of a Haptic Display," in *Proceedings of the 1994 IEEE International Conference on Robotics and Automation*, vol. 4, San Diego, CA, USA, May 1994, pp. 3205–3210.

[36] B. Hannaford and J. H. Ryu, "Time-Domain Passivity Control of Haptic Interfaces," *IEEE Transactions on Robotics and Automation*, vol. 18, no. 1, pp. 1–10, February 2002.

[37] J. J. Abbott and A. M. Okamura, "Effects of Position Quantization and Sampling Rate on Virtual-Wall Passivity," *IEEE Transactions on Robotics*, vol. 21, no. 5, pp. 952–964, October 2005.

[38] K. J. Kuchenbecker, J. Fiene, and G. Niemeyer, "Improving Contact Realism throug E]vent-Based Haptic Feedback, journal=IEEE Transactions on Visualization and Computer Graphics, volume=13, number=2, pages=219-230, year=2006, month=March/April,."

[39] A. Abdossalami and S. Sirouspour, "Adaptive Control for Improved Transparency in Haptic Simulations," *IEEE Transactions on Haptics*, vol. 2, no. 1, pp. 2–14, January-March 2009.

[40] D. Wang, K. Tuer, M. Rossi, L. Ni, and J. Shu, "The Effect of Time Delays on Tele-Haptics," in *Proceedings of the 2nd IEEE International Workshop on Haptic, Audio and Visual Environments and Their Applications*, September 2003, pp. 7–12.

[41] J. Kim, H. Kim, B. K. Tay, M. Muniyandi, M. A. Srinivasan, J. Jordan, J. Mortensen, M. Oliveira, and M. Slater, "Transatlantic Touch: A Study of Haptic Collaboration over Long Distance," *Presence: Teleoperators and Virtual Environments*, vol. 13, no. 3, pp. 328–337, June 2004.

[42] J. Zhou, X. Shen, A. E. Saddik, and N. D. Georganas.

[43] T. Hulin, C. Preusche, and G. Hirzinger, "Stability Boundary for Haptic Rendering: Influnce of Human Operator," in *2008 IEEE/RSJ International Conference on Intelligent Robots and Systems*, Nice, France, September 2008, pp. 3483–3488.

[44] S. Ferrari and Y. Hu, "The Effect of Incongruent Delay on Guided Haptic Training," in *IEEE World Haptics Conference 2011*, Istanbul, Turkey, June 2011, pp. 161–166.

[45] J. R. Cooper, M. M. Wernke, and K. B. Reed, "The Effects of Incongruent Feedback on Bimanual Task Performance," in *Haptics Symposium 2012*, Vancouver, BC, Canada, March 2012, pp. 301–305.

[46] N. Diolaiti and G. Niemeyer, "Wave Haptics: Providing Stiff Coupling to Virtual Environments," in *2006 14th Symposium on Haptic Interfaces for Virtual Environment and Teleoperator Systems*, Alexandria, VA, USA, March 2006, pp. 185–192.

[47] M. Alise, R. G. Roberts, and D. W. Repperger, "Implementation of the Wave Variable Method on a PHANTOM Omni Haptic Device," in *2006 Florida Conference on Recent Advances in Robotics, FCRAR 2006*, Miami, FL, USA, May 2006.

[48] Y. Ye and P. X. Liu, "Improving Haptic Feedback Fidelity in Wave-Variable Based Teleoperation Oriented to Telemedical Application," *IEEE Transactions on Instrumentation and Measurement*, vol. 58, no. 8, pp. 2847–2855, August 2009.

[49] M. Alise, R. G. Roberts, D. W. Repperger, and J. C. A. Moore, "A Haptic Teleoperation Study using Wave Variables and Scaling Matrices," in *Proceedings of the 2009 IEEE International Conference on Systems, Man and Cybernetics*, San Antonio, TX, USA, October 2009.

[50] N. Yasrebi and D. Constantinescu, "Passive Wave Variable Control of Haptic Interaction with an Unknown Virtual Environment," in *Proceedings of the 2011 IEEE*

International Conference on Robotics and Automation, Shanghai, China, May 2011, pp. 919–924.

[51] I. G. Polushin, P. X. Liu, and C. H. Lung, "A Force-Reflection Algorithm for Improved Transparency in Bilateral Teleoperation With Communication Delay," *IEEE/ASME Transactions on Mechatronics*, vol. 12, no. 3, pp. 361–374, June 2007.

[52] ——, "Projection-Based Force Reflection Algorithm for Stable Bilateral Teleoperation over Networks," in *The 2007 IEEE/RSJ International Conference on Intelligent Robots and Systems*, San Diego, USA, October-November 2007, pp. 2654–2659.

[53] ——, "Stability of Bilateral Teleoperators with Projection-Based Force Reflection Algorithm," in *The 2008 IEEE/RSJ International Conference on Robotics and Automation*, Pasadena, CA, USA, May 2008, pp. 677–682.

[54] ——, "Projection-Based Force Reflection Algorithm for Stable Bilateral Teleoperation over Networks," *IEEE Transactions on Instrumentation and Measurements*, vol. 57, no. 9, pp. 1854–1865, September 2008.

[55] ——, "Experimental Studies of a Teleoperator System with Projection-Based Force Reflection Algorithms," in *The 2009 IEEE/RSJ International Conference on Intelligent Robots and Systems*, St. Louis, IL, USA, October 2009, pp. 5127–5132.

[56] I. G. Polushin, A. Takhmar, and R. V. Patel, "Small Gain Design of Cooperative Teleoperator System with Projection Based Force Reflection," in *2011 IEEE/RSJ International Conference on Intelligent Robots and Systems*, San Francisco, CA, USA, September 2011, pp. 653–658.

[57] J. E. Colgate, P. E. Grafing, M. C. Stanley, and G. Schenkel, "Implementation of Stiff Virtual Walls in Force-reflecting Interfaces," in *Virtual Reality Annual International Symposium*, 1993, pp. 202–208.

[58] M. Minsky, M. O. Young, O. Steele, J. F. P. Brooks, and M. Behensky, "Feeling and Seeing: Issues in Force Display," in *Proceedings of the 1990 Symposium on Interactive 3D Graphics*, Snowbird, UT, USA, February 1990, pp. 235–241.

[59] J. E. Colgate and G. G. Schenkel, "Passivity of a Class of Sampled-Data Systems: Application to Haptic Interfaces," *Journal of Robotic Systems*, vol. 14, no. 1, pp. 37–47, 1997.

[60] G. Niemeyer and J. J. E. Slotine, "Stable Adaptive Teleoperation," *IEEE Journal of Oceanic Engineering*, vol. 16, no. 1, pp. 152–162, January 1991.

[61] ——, "Telemanipulation with Time Delays," *The International Journal of Robotics Research*, vol. 23, no. 9, pp. 873–890, September 2004.

[62] N. A. Tanner and G. Niemeyer, "Improving Perception in Time-delayed Telerobotics," *The International Journal of Robotics Research*, vol. 24, no. 8, pp. 631–644, August 2005.

[63] "Class lectures," ECE9510: Telerobotics, Summer 2010, university of Western Ontario.

[64] G. Niemeyer and J. J. E. Slotine, "Towards Force-Reflecting Teleoperation Over the Internet," in *Proceedings of the 1998 IEEE Internaional Conference on Robotics and Automation*, Leuven, Belgium, May 1998, pp. 1909–1915.

[65] I. G. Polushin, P. X. Liu, and C. H. Lung, "A Control Scheme for Stable Force-Reflecting Teleoperation over ip Networks," *Systems, Man, and Cybernetics, Part B: Cybernetics, IEEE Transactions on*, vol. 36, no. 4, pp. 930 –939, August 2006.

[66] T. B. Sheridan, "Space Teleoperation Through Time Delay: Review and Prognosis," *IEEE Transactions on Robotics and Automation*, vol. 9, no. 5, pp. 592–606, October 1993.

[67] A. Stotsky and I. Kolmanovsky, "Application of Input Estimation Techniques to Charge Estimation and Control in Automotive Engines," *Control Engineering Practice*, vol. 10, no. 12, pp. 1371–1383, December 2002.

Appendix A

Dirty Derivative Filter

A dirty derivative filter [65] has been used to obtain the estimate of velocity from position information. The filter design consists of the following equations:

$$\dot{\xi}_1 = \xi_2 + g\alpha_1(\hat{q}_m - \xi_1) \tag{A.1}$$

$$\dot{\xi}_2 = g^2\alpha_0(\hat{q}_m - \xi_1) \tag{A.2}$$

α_0 and α_1 are positive constants such that the roots of $p(s) = s^2 + \alpha_1 s + \alpha_0$ have negative real parts and g is a positive constant and is the gain of the filter. The cut-off frequency of this filter can be found as follows,

$$f_{c_{dd}} = \sqrt{\alpha}g \tag{A.3}$$

and will have an unit of rad/s. $\hat{q}_m$ in the above equations is the reference signal and is an estimate of the position. The introduction of the dirty derivative filter serves two purposes:

1. If $\hat{q}_m$ is sufficiently smooth, the filter serves as a reduced order observer and provides the first and second order time derivatives of $\hat{q}_m$ (velocity ξ_2 and $\dot{\xi}_2$).

2. If $\hat{q}_m$ is not sufficiently smooth (discontinuous), the filter acts as a governor to provide a smooth approximation.

Appendix B

High Gain Observer

Considering a first-order dynamic system

$$\dot{z} = y + x \tag{B.1}$$

where, the signals z and y are measured. The time varying input x is unknown and needs to be estimated online. In order to make a measurement of x, a controller can be designed for the system such that,

$$\dot{\hat{z}} = u \tag{B.2}$$

using the virtual control variable u to estimate x since,

$$y + x = u \tag{B.3}$$

This class of controllers are referred to as observers. One of the popular types of observers is high gain observer [67]. It is defined in terms of the auxiliary variables v and ϵ, where,

$$v = \gamma z - \epsilon - x \tag{B.4}$$

and ϵ satisfies,

$$\dot{\epsilon} = -\gamma\epsilon + \gamma y + \gamma^2 z \tag{B.5}$$

where $\gamma > 0$ is the observer gain. By increasing the value of gain γ, the value of the error v can be made arbitrarily small [67], thereby making the estimate $\hat{x}$ more accurate. This estimate can be found from,

$$\hat{x} = \gamma z - \epsilon \tag{B.6}$$

Another way to find the same solution is to filter both sides of the system equation using a low-pass filter. The filtered equation will be,

$$\frac{1}{\tau s + 1} x = \frac{1}{\tau s + 1}(sz - y) \tag{B.7}$$

where, τ is the filter time constant and $s = j\omega$ is the Laplace variable. Now, from the above equation,

$$\begin{aligned} \frac{1}{\tau s + 1} x &= \frac{z}{\tau} - \frac{1}{\tau s + 1}(\frac{z}{\tau} + y) \\ &= \frac{z}{\tau} - \epsilon \end{aligned} \tag{B.8}$$

where, ϵ is denoted as,

$$\epsilon = \frac{1}{\tau s + 1}(\frac{z}{\tau} + y) \tag{B.9}$$

So, the estimate of x can be found as

$$\hat{x} = \frac{1}{\tau} z - \epsilon \tag{B.10}$$

With $\gamma = \frac{1}{\tau}$, it is reduced to the earlier equation for the estimate of x.

Appendix C

Model of the Phantom Omni^{TM} Haptic Device

Figure C.1: Phantom Omni from SensAble Inc. [2]

The Phantom Omni^{T}M haptic device can be represented by a dynamic equation of the following form:

$$M(\theta)\ddot{\theta} + C(\theta, \dot{\theta})\dot{\theta} + G(\theta) + K_F(\dot{\theta}) = J^T(\theta)f_h - J^T(\theta)f_r \tag{C.1}$$

In the dynamic equation,

$M(\theta)$ = 3×3 matrix of inertia,

$C(\theta, \dot{\theta})$ = 3×3 matrix of Coriolis and centrifugal forces

$G(\theta)$ = 3×1 gravity vector

$K_F(\dot{\theta})$ = dissipative torques

f_h = force applied by the human operator

f_r = reflected force

$J(\theta)$ = Jacobian of the device

The elements of the matrices and vectors are defined as follows:

$M_{11} = \pi_1 + \pi_2 \cos^2(\theta_2) + (\pi_3 + \pi_5)\sin^2(\theta_3) + 2\pi_6 \cos(\theta_2)\sin(\theta_3)$

$M_{22} = \pi_4 + \pi_5 - 2\pi_6 \sin(\theta_2 - \theta_3)$

$M_{23} = M_{32} = \pi_5 - \pi_6 \sin(\theta_2 - \theta_3)$

$M_{33} = \pi_5$ $C_{11} = -(\pi_2 \sin(\theta_2)\cos(\theta_2) + \pi_6 \sin(\theta_2)\sin(\theta_3))\dot{\theta}_2 + ((\pi_3 + \pi_5)\sin(\theta_3)\cos(\theta_3) + \pi_6 \cos(\theta_2)\cos(\theta_3))\dot{\theta}_3$

$C_{12} = -(\pi_2 \sin(\theta_2)\cos(\theta_2) + \pi_6 \sin(\theta_2)\sin(\theta_3))\dot{\theta}_3$

$C_{13} = ((\pi_3 + \pi_5)\sin(\theta_3)\cos(\theta_3) + \pi_6 \cos(\theta_2)\cos(\theta_3)\dot{\theta}_1$

$C_{21} = (\pi_2 \sin(\theta_2)\cos(\theta_2) + \pi_6 \sin(\theta_2)\sin(\theta_3))\dot{(\theta_1)}$

$C_{22} = \pi_6 \cos(\theta_2 - \theta_3)(\dot{(\theta_3)} - \dot{(\theta_2)})$

$C_{23} = \pi_6 \cos(\theta_2 - \theta_3)(\dot{\theta}_2 - \dot{\theta}_3)$

$C_{31} = (-(\pi_3 + \pi_5)\sin(\theta_3)\cos(\theta_3) - \pi_6 \cos(\theta_2)\cos(\theta_3))\dot{\theta}_1$

$C_{32} = -2\pi_6 \cos(\theta_2 - \theta_3)\dot{\theta}_2$

$C_{33} = 0$

$G_1 = 0$

$G_2 = \pi_7 \cos(\theta_2)$

$G_3 = \pi_8 \sin(\theta_3)$

$K_{F1} = \pi_9 \dot{\theta}_1 + \pi_{12} \tanh(\dot{\theta}_1)$

$K_{F2} = \pi_{10} \dot{\theta}_2 + \pi_{13} \tanh \dot{\theta}_2$

$K_{F3} = \pi_{11} \dot{\theta}_3 + \pi_{14} \tanh \dot{\theta}_3$

The least-squares parameter identification algorithm was used to determine the parameters

$\pi_1 \ldots \pi_{14}$, which are the parameters of the device. The values of these parameters are given below.

$$\pi = \begin{bmatrix} \pi_1 \\ \pi_2 \\ \pi_3 \\ \pi_4 \\ \pi_5 \\ \pi_6 \\ \pi_7 \\ \pi_8 \\ \pi_9 \\ \pi_{10} \\ \pi_{11} \\ \pi_{12} \\ \pi_{13} \\ \pi_{14} \end{bmatrix} = \begin{bmatrix} 0.00001 \\ 0.0028 \\ 0.0005 \\ 0.0009 \\ 0.0002 \\ 0.0010 \\ 0.0805 \\ 0.1184 \\ 0.0048 \\ 0.0099 \\ -0.0017 \\ 0.0203 \\ 0.0305 \\ 0.0313 \end{bmatrix} \tag{C.2}$$

Curriculum Vitae

Name:	Mir Zayed Hasan
Post-Secondary Education and Degrees:	University of Dhaka, Dhaka, Bangladesh 1996 - 2000 B.Sc. University of Dhaka, Dhaka, Bangladesh 2000 - 2001 M.S.
Related Work Experience:	Teaching Assistant The University of Western Ontario 2011 - 2012

Publications:

1. Ilia Polushin, Mir Zayed Hasan, Amir Takhmar, *Experimental Evaluation of a Projection-based Force Reflection Algorithm for Haptic Interfaces*, 2012 Haptics Symposium, pp. 503-507, 4-7 March 2012, Vancouver, British Columbia, Canada.

2. Mir Zayed Hasan, *Projection based Force Reflection Algorithm for Rendering Stiff Virtual Environments*, Tenth International Conference for Upcoming Engineers (ICUE 2011), pp 43-46, May, 2011, Toronto, Ontario, Canada.